ADVISORY GROUP FOR AERONAUTICAL
RESEARCH AND DEVELOPMENT

REPORT 276

ON SURFACE PRESSURE FLUCTUATIONS IN TURBULENT BOUNDARY LAYERS

by

G. M. LILLEY and T. H. HODGSON

APRIL 1960

NORTH ATLANTIC TREATY ORGANISATION
64 RUE DE VARENNE, PARIS VII

REPORT 276

NORTH ATLANTIC TREATY ORGANIZATION

ADVISORY GROUP FOR AERONAUTICAL RESEARCH AND DEVELOPMENT

ON SURFACE PRESSURE FLUCTUATIONS IN TURBULENT BOUNDARY LAYERS

by

G.M. Lilley and T.H. Hodgson

This Report is one in the Series 253-284 of papers presented at the Boundary Layer Research Meeting of the AGARD Fluid Dynamics Panel held from 25th to 29th April 1960, in London, England

SUMMARY

Existing work on the pressure fluctuations in turbulent shear flows is briefly reviewed with special reference to the problem of wall turbulence.

An approximate theory for the pressure fluctuations on the wall under both a turbulent boundary layer and a wall jet is given and indicates in the latter case an intensity many times that corresponding to the flow over a flat plate at zero pressure gradient, as typified by measurements on the wall of a wind tunnel. Experiments on a wall jet confirm these predictions and details of the few preliminary data are presented.

The results from the wall jet suggest that the intensity of the pressure fluctuations in the regions of adverse pressure gradient, on wings and bodies, approaching and beyond separation will be higher than in regions of zero pressure gradient.

Appendices are included which deal with the necessary extensions to the analysis to fit the velocity correlation functions as measured by Grant (1958), the effects of time delay and eddy convection.

SOMMAIRE

Les travaux effectués jusqu'ici sur les variations de pression dans un écoulement turbulent en cisaillement sont sommairement exposés avec mention particulière du problème de la turbulence à la paroi.

Les auteurs présentent une théorie approchée pour les variations de pression à la paroi sous l'influence tant d'une couche limite turbulente que d'un jet à la paroi, d'après laquelle, dans ce dernier cas, les variations de pression sont sensiblement plus fortes que celles qui correspondent à l'écoulement sur une plaque plane en l'absence de gradients de pression, ainsi que le démontrent les mesures effectuées sur la paroi d'un soufflerie. Cette prédiction est confirmée par les résultats d'essais sur un jet à la paroi; les quelques résultats préliminaires obtenus sont présentés ici.

Ces résultats font penser que l'intensité des variations de pression dans les régions à gradients défavorables, par exemple, sur les ailes et les corps, quand l'écoulement s'approche du point de décollement et passe au-delà, sera plus forte que dans les régions à gradients nuls.

Le rapport comprend des annexes traitant des extensions à apporter à l'analyse pour la rendre applicable aux fonctions de la corrélation des vitesses, ainsi qu'elles ont été mesurées par Grant en 1958, à l'influence du retard temporel et à la convection des tourbillons.

3b2c2d:3b2e1a4a

532.526.4

CONTENTS

LIST OF FIGURES

NOTATION

A	amplitude
a_1, a_2, a_3	amplitude of big eddy velocity covariances
c_f	skin friction coefficient ($\equiv \tau_w / \frac{1}{2}\rho u_m^2$)
D	jet diameter
f	longitudinal velocity correlation coefficient (isotropic turbulence)
G, G_0, G_1, G_+, G_-	Green's functions
K	von Kármán constant
l, l_p, l_1, l_2	scales of turbulence
P	pressure covariance
$\bar{P}$	pressure spectrum function
p	pressure
$\sqrt{\overline{p^2}}$	r.m.s. value of pressure fluctuations
q	source density
R, Φ, Z	cylindrical polar co-ordinates
R_{ij}, R_{ZZ}	velocity covariance
$\bar{R}_{ij}, \bar{R}_{ZZ}$	velocity correlation coefficient
$\vec{r}$	$\equiv (r_1, r_2, r_3)$
$\vec{r}'$	$\equiv (r_1', r_2', r_3', r_4')$
S	area
t	time
(u_R, u_Φ, u_Z)	velocity components
$\bar{U}_R, \bar{U}_\Phi, \bar{U}_Z$	mean velocity components
$\vec{u}$	velocity ($\equiv (u_1, u_2, u_3)$)
u_τ	maximum velocity at a given R
u_∞	free stream velocity

u_τ	shear velocity
$\bar{u}_c$	convection speed
V	volume
$\vec{x}$, $\vec{y}$, $\vec{z}$	co-ordinates
$Z_{1/2}$, Z_m	distance to mid and maximum velocity in the outer region respectively
a	$\overline{u_Z^2}/u_\tau^2$, and anisotropy factor
a_1, a_2, a_3	reciprocals of typical turbulence scales
δ	Dirac function; boundary layer thickness
δ_1	displacement thickness
κ	wave number
μ	viscosity
ν	kinematic viscosity; reciprocal of eddy lifetime
$\vec{\xi}$	$\vec{x}' - \vec{x}$
ρ	density
τ	time delay
τ, τ_{RZ}	mean shear
τ_m	optimum time delay
τ_w	wall shear stress
ω	circular frequency
$(\ )_b$	denotes big eddy contribution
$(\ )_s$	denotes small eddy contribution
$^{\neg}(\ )$	denotes 'in moving frame of reference'
$^{f}(\ )$	denotes 'in fixed frame of reference'
$'$	denotes fluctuating quantities (but generally omitted)

ON SURFACE PRESSURE FLUCTUATIONS IN TURBULENT BOUNDARY LAYERS

G.M. Lilley and T.H. Hodgson*

1. INTRODUCTION

A knowledge of the intensity and spectra of the pressure fluctuations in turbulent shear flows is required in a wide range of aeronautical and hydrodynamic problems today. Such problems range from aerodynamic noise generated by turbulent motion, the vibrations of the aircraft skin at high speeds and the transmission of noise to the cabin and cockpit, to mention just a few.

Although work in this area was pioneered by Heisenberg[1], Obukhoff[2], Batchelor[3] and Kraichnan[4,5], it is only relatively recently that experimental data have been obtained to check the theoretical data, and to set the pattern for investigations into more complicated situations, where the theory at best would be very tentative. The work of Kraichnan is of particular interest for it deals with pressure fluctuations in the presence of a mean shear, and also in the case of wall turbulence, and therefore has direct application to the problem of wall pressure fluctuations under a turbulent boundary layer. (The earlier work of Heisenberg, Obukhoff and Batchelor considered only the case of isotropic turbulence). Kraichnan showed that on a wall $\sqrt{\overline{p^2}}/(\frac{1}{2}\rho u_m^2) \sim \beta c_f$, where β is a factor between 2 and 12. Experimental results obtained by Willmarth[6] and Harrison[7] confirmed Kraichnan's predictions and gave values of β between 2.5 and 5.0.

The effect of Mach number on wall pressure fluctuations, although of obvious current importance, will not be considered here. Indeed, the flow will be assumed incompressible throughout and the problem of boundary layer noise, that is the noise radiated away from the surface, will hardly be touched upon. Our attention will mainly be restricted to problems of wall turbulence, including the wall jet, and will not consider in the same detail pressure fluctuations in free turbulence. A review paper covering the items omitted by the authors would naturally be of considerable topical interest, but it was felt that, bearing in mind the considerable efforts present in this area today and the present state of flux of knowledge in the subject, a greater need was for a fundamental appreciation of relatively simple flow models. The surface over which the fluid flows will be treated as rigid, and no account will be given of the response of the structure to pressure fluctuations.

The theory of the pressure fluctuations in wall turbulence, including the wall jet, will be treated on similar lines to the method used by Kraichnan[5]. In this method the intensity of the pressure fluctuations can be obtained once the two-point velocity correlations, mean velocity gradient, and the turbulence intensity and scale are known. Experimental results obtained by Townsend[8], Laufer[9], and Grant[10] will be used to find $\overline{p^2}$ on the wall. For the wall jet the mean flow theory due to Glauert[11] will be adopted, together with results in the mean flow by Bakke[12] and Bradshaw and Love[13]. The prediction in this case for $\overline{p^2}$ will be compared with those obtained from measurements.

---

*Department of Aerodynamics, College of Aeronautics, Cranfield, England

Finally, in order to avoid confusion in the theoretical treatment and the discussion of results, the authors stress that they are dealing with the problem of pressure fluctuations in a pseudo-incompressible turbulent shear flow. They prefer, and agree that it is one of personal preference and not one agreed by convention, to refer to boundary layer noise as the sound energy radiated away from the turbulent flow. This latter problem, considered by Curle[14], Phillips[15], and Doak[16], though connected, has obvious differences from the present treatment.

2. THEORY OF THE PRESSURE FLUCTUATIONS IN A SHEAR FLOW

In most instances where the pressure fluctuations are significant the fluctuations in the fluid density are significant also. The present problem is no exception. However, since we will be more concerned with the pressure fluctuations inside the turbulent shear flow, which in our problem will be an essentially 'low speed flow', than with the noise radiated from it, we may safely assume that the flow is incompressible. The equations of continuity and motion are therefore respectively

$$\frac{\partial u_i}{\partial x_i} = 0 \tag{1}$$

$$\frac{\partial \rho u_i}{\partial t} + \frac{\partial}{\partial x_j} \rho u_i u_j = - \frac{\partial p}{\partial x_i} + \mu \nabla^2 u_i \tag{2}$$

If we take the divergence of (2) and use (1) we obtain the following equation for the pressure:

$$\nabla^2 p = - \rho \frac{\partial^2 u_i u_j}{\partial x_i \partial x_j} \tag{3}$$

This shows that, whereas in inviscid steady flow the pressure at a point follows immediately from the dynamic pressure at the same point, the pressure at a point in a turbulent flow, since it obeys an equation of the Poisson type, is governed by fluctuations in velocity throughout the entire flow and not just at the field point. Since the wall jet comprises an inner boundary layer and an outer jet mixing region we will, for convenience in finding the solution to (3), consider this more general flow only. The solution for the boundary layer on a flat plate is then a particular case.

In the wall jet the mean pressure is approximately constant everywhere, and the mean velocity field is radially symmetric so that in terms of cylindrical polar co-ordinates (R, ϕ, Z), the velocity components are given by $\bar{u}_R(R, Z)$, $\bar{u}_\phi = 0$ and $\bar{u}_Z(R, Z)$.

Since Equation (3) above can be written alternatively in vector notation as

$$\nabla^2 p = - \rho \nabla \cdot (\vec{u} \cdot \nabla) \vec{u} \tag{3a}$$

we find on expanding the right hand side and making the usual boundary layer assumption that (see Appendix A)

$$\nabla^2 p \;\triangleq\; -\rho\left(\frac{\partial u_R'}{\partial R}\frac{\partial \bar{u}_R}{\partial R} + 2\frac{\partial u_Z'}{\partial R}\frac{\partial \bar{u}_R}{\partial Z}\right) \tag{4}$$

where (u_R', u_ϕ', u_Z') denote the fluctuating components of velocity and $(\bar{u}_R, \bar{u}_\phi, \bar{u}_Z)$ the mean values.

But $\dfrac{\partial \bar{u}_R}{\partial R} \ll \dfrac{\partial \bar{u}_R}{\partial Z}$ so that finally we have

$$\nabla^2 p \;=\; -2\rho\frac{\partial u_Z'}{\partial R}\frac{\partial \bar{u}_R}{\partial Z} \tag{5}$$

$$\;=\; -2\rho\,\tau_{RZ}\frac{\partial u_Z'}{\partial R} \tag{5a}$$

where $\tau_{RZ}(R,Z) \;\equiv\; \dfrac{\partial \bar{u}_R}{\partial Z}$ is the local mean shear.

This result is similar to that found by Kraichnan[5] for the boundary layer flow over a flat plate with a mean velocity in the (x_1) direction varying with (x_2) only, the direction normal to the plate.

In order to simplify the notation, in what follows, we will drop the subscripts on τ and the primes on u_Z. Thus p and $\vec{u}$ will *now* refer to the fluctuating pressure and velocity respectively, and τ is the mean shear. Therefore we can write Equation (5a) in the equivalent form

$$\nabla^2 p \;=\; -2\rho\tau\frac{\partial u_Z}{\partial R} \;=\; -q(\vec{x},\,t) \tag{6}$$

where $q(\vec{x},\,t)$ is the source density. We are here assuming that the pressure fluctuations due to the amplifying effect of the mean shear on the turbulence are greater than that due to the interaction of the turbulence on itself. Kraichnan[5] justifies the use of this assumption by showing that, approximately, the former will give rise to a root mean square value of pressure about 10 db higher over that due to the latter.

The solution of (6) can be found by finding an appropriate Green function, $G(\vec{x},\,\vec{x}')$, which satisfies the boundary conditions. Since the Green function satisfies

$$\nabla^2 G(\vec{x},\,\vec{x}') \;=\; -\delta(\vec{x}-\vec{x}') \tag{7}$$

where $\delta(y)$ is the Dirac delta function, the appropriate solution of (6) is

$$p(\vec{x},\,t) \;=\; \int_V q(\vec{y},\,t)\,G(\vec{x},\,\vec{y})\,d\vec{y} + \int_S G\frac{\partial p}{\partial n}(\vec{y},\,t) - p(\vec{y},\,t)\frac{\partial G}{\partial n}\,dS(\vec{y}) \tag{8}$$

where V is the total volume occupied by the flow and S is the total area of the plane over which the fluid flows, provided that at some initial time p and $\partial p/\partial t$ vanish. Here n is the normal to S, measured to the surface from the volume.

If we write G_- the Green function which vanishes on the plane S, G_+ the Green function given by

$$\frac{\partial G_+}{\partial n} = 0$$

on the plane S, and G_0 the Green function for unbounded space, we have

$$\left.\begin{aligned} G_- &= G_0 - G_i \\ G_+ &= G_0 + G_i \end{aligned}\right\} \tag{9}$$

where G_i is the Green function for the image point in the boundary. Hence we can find three equivalent solutions of (6), which depend on the particular choice of Green function. Thus

$$p(\vec{x}, t) = \int_V q\, G_+\, dV + \int_S G_+ \frac{\partial p}{\partial n}\, dS \tag{10a}$$

$$= \int_V q\, G_-\, dV - \int_S p \frac{\partial G_-}{\partial n}\, dS \tag{10b}$$

$$= \int_V q\, G_0\, dV + \int_S \left(G_0 \frac{\partial p}{\partial n} - p \frac{\partial G_0}{\partial n} \right) dS \tag{10c}$$

But on S we have

$$\left.\begin{aligned} G_0 &= G_i \\ \frac{\partial G_0}{\partial n} &= -\frac{\partial G_i}{\partial n} \end{aligned}\right\} \tag{11}$$

and so (10) can be written alternatively

$$p(\vec{x}, t) = \int_V q(G_0 + G_i)dV + 2\int_S G_0 \frac{\partial p}{\partial n}\, dS \tag{12a}$$

$$= \int_V q(G_0 - G_i)dV - 2\int_S p \frac{\partial G_0}{\partial n}\, dS \tag{12b}$$

$$= \int_V q\, G_0\, dV + \int_S \left(G_0 \frac{\partial p}{\partial n} - p \frac{\partial G_0}{\partial n} \right) dS \tag{12c}$$

The particular choice of one of these equations must depend on what is known about p and $\partial p/\partial n$ on the plane S. Clearly if $\partial p/\partial n = 0$ on S we would choose (12a).

Now the equation of motion in the Z-direction at Z = 0, where $u_R = u_\phi = u_Z = 0$, is

$$0 = -\frac{\partial p}{\partial Z} + \mu \frac{\partial^2 u_Z}{\partial Z^2} \tag{13}$$

for the fluctuating quantities and

$$0 = \mu \frac{\partial^2 \bar{u}_Z}{\partial Z^2} \tag{14}$$

for the mean flow.

But from the equation of continuity

$$\frac{\partial \bar{u}_Z}{\partial Z}, \quad \frac{\partial u_Z}{\partial Z} = 0 \quad \text{at} \quad Z = 0 \tag{15}$$

and therefore near the wall

$$\overline{u_Z^2} = \frac{Z^4}{4\mu^2}\overline{\left(\frac{\partial p}{\partial Z}\right)^2} + \ldots\ldots \tag{16}$$

From the measured distribution of $\overline{u_Z^2}$ near the wall of a flat plate, channel or pipe Townsend[6] finds that (in our notation),

$$\overline{\left(\frac{\partial p}{\partial Z}\right)^2} \approx 3.4 \times 10^{-3} \frac{\tau_w^3}{\rho\nu^2} \tag{17}$$

where $\tau_w(R)$ is the wall mean shear stress given by

$$\tau_w \equiv \left(\mu \frac{\partial \bar{u}_R}{\partial Z}\right)_{Z=0} \tag{18}$$

Although $\overline{(\partial p/\partial Z)^2}$, as shown by (17), is a very small quantity we are not immediately justified in putting $(\partial p/\partial Z)_{Z=0} = 0$ in (12a).

However, if l_1 is a typical length over which the velocity is correlated and l_2 a similar length with respect to pressure, we see that the contributions to $\overline{p^2}$, from the volume and surface integrals in (12a), are in the ratio

$$100\, l_1^2 \quad : \quad l_2^2$$

Now, if anything, l_2 is less than l_1 and is certainly not large compared with l_1, and so we see that the surface integral in (12a) can be neglected in agreement with Kraichnan's approximation[5]. Thus we note that for this problem the solutions (12b) and (12c) are of less value than the first.

We therefore write approximately

$$p(\vec{x},\ t) \ = \ \frac{\rho}{2\pi} \int_V (|\vec{x} - \vec{y}|^{-1} + |\vec{x} - \vec{y}^*|^{-1})\ \tau(\vec{y})\ \frac{\partial u_Z}{\partial y_R}\ (\vec{y})\ d\vec{y} \tag{19}$$

on inserting $q(\vec{x},\ t)$ from (6) into (12a), and noting that

$$G_0 - G_1 \ = \ \frac{1}{4\pi}\left(\frac{1}{|\vec{x} - \vec{y}|} - \frac{1}{|\vec{x} - \vec{y}^*|}\right) \tag{20}$$

where $\vec{y} \equiv (y_R,\ y_\phi,\ y_Z)$; $\vec{y^*} \equiv (y_R,\ y_\phi,\ -y_Z)$, and the volume of integration is over the half-space $Z > 0$.

On the surface of the plane $\vec{x} \equiv (R,\ \phi,\ 0)$ so that

$$p(\vec{x},\ t)_{Z=0} \ = \ \frac{\rho}{\pi} \int_{Z>0} \frac{\tau(\vec{y})\ \dfrac{\partial u_Z}{\partial y_R}\ (\vec{y})}{|\vec{x} - \vec{y}|}\ d\vec{y} \tag{21}$$

and the pressure covariance, for zero time delay between the pressures on the plane at $\vec{x}$ and $\vec{x}'$ respectively, is

$$P(\vec{x};\ \vec{x}')_{Z=0} \ = \ \frac{\rho^2}{\pi^2} \int_{Z',\,Z>0} \int \frac{\tau(\vec{y})\ \tau(\vec{z})\ \dfrac{\partial^2 R_{ZZ}}{\partial y_R\ \partial z_R}\ d\vec{y}\ d\vec{z}}{|\vec{x} - \vec{y}|\ \ |\vec{x}' - \vec{z}|} \tag{22}$$

where the velocity covariance is

$$R_{jl} \ = \ \overline{u_j'(\vec{y})\ u_l\ (\vec{z})}$$

and $\vec{Z} \equiv (Z_R,\ Z_\phi,\ Z_Z)$.

If the turbulence is spatially locally homogeneous we can put

$$\frac{R_{ZZ}\ (\vec{y}\ ;\ \vec{z})}{\sqrt{\overline{u_Z^2}\ (\vec{y})}\ \sqrt{\overline{u_Z^2}\ (\vec{z})}} \ = \ \bar{R}_{ZZ}\ (\vec{r}) \tag{23}$$

where $\vec{r} \equiv (\vec{z} - \vec{y})$ and $\bar{R}_{ZZ}$ is the velocity correlation coefficient.

Now the integral in Equation (22) with (23) is difficult to evaluate for general values of τ and $\overline{u_Z^2}$. However, the contributions to the integral beyond a certain distance of the order of the length scale of the turbulence will be sufficiently small so that τ and $\overline{u_Z^2}$ can be regarded as functions of $|\vec{x}|$ and y_Z only. This assumption means that so far as the integral in (22) is concerned τ and $\overline{u_Z^2}$ vary only with distance normal to the plane and, in view of the locally homogeneous assumption in (23), the integral can be evaluated as if the flow were parallel. For convenience in its

evaluation we will use a rectangular cartesian tensor notation with y_1 and y_3 taken in the plane of the wall and y_2 normal to the wall. Thus (22) becomes

$$P(\vec{x};\ \vec{x}')_{Z=0} = -\frac{\rho^2}{\pi^2}\int_{-\infty}^{\infty} dy_1 \int_{0}^{\infty} dy_2 \int_{-\infty}^{\infty} dy_3 \int_{-\infty}^{\infty} dr_1 \int_{-y_2}^{\infty} dr_2 \int_{-\infty}^{\infty} dr_3 \frac{\tau(\vec{x};y_2)\ \tau(\vec{x};y_2+r_2)}{|\vec{x}-\vec{y}|\ |\vec{x}'-\vec{y}-\vec{r}|}$$

$$\cdot\sqrt{\overline{u_2^2}}\,(\vec{x};y_2)\sqrt{\overline{u_2^2}}\,(\vec{x};y_2+r_2)\frac{\partial^2 \bar{R}_{22}}{\partial r_1^2}(\vec{r}) \qquad (24)$$

If $\bar{R}_{22}$ and its derivatives with respect to r_1 vanish at infinity an integration by parts of (24) leads to

$$P(\vec{x};\ \vec{x}')_{Z=0} = \frac{\rho^2}{\pi^2}\int_{-\infty}^{\infty} dy_1 \int_{0}^{\infty} dy_2 \int_{-\infty}^{\infty} dy_3 \int_{-\infty}^{\infty} dr_1 \int_{-y_2}^{\infty} dr_2 \int_{-\infty}^{\infty} dr_3\ \bar{R}_{22}(\vec{r})$$

$$\tau(\vec{x};\ y_2)\ \tau(\vec{x};\ y_2+r_2)\sqrt{\overline{u_2^2}}\,(\vec{x};\ y_2)\sqrt{\overline{u_2^2}}\,(\vec{x}_2;\ y_2+r_2)$$

$$\frac{\partial}{\partial y_1}\left(\frac{1}{|\vec{x}-\vec{y}|}\right)\frac{\partial}{\partial z_1}\left(\frac{1}{|\vec{x}'-\vec{z}|}\right) \qquad (25)$$

Now it must be noted that in this analysis stationary, and *not* moving co-ordinates are being used. Also, as stated above, $P(\vec{x};\ \vec{x}')$, the pressure covariance on the plane $Z = 0$, is that for zero time delay and involves the instantaneous product of the fluctuating pressures at the points $\vec{x}$ and $\vec{x}'$ respectively. However, if the frequency spectrum of the wall pressure fluctuations is required it is necessary to consider both the time delay and the turbulence in a moving frame of reference (see Appendices D and E).

Equation (25) is the important equation in this paper. It shows that the pressure covariance at a point on the wall, due to shear flow turbulence dominated by the mean flow shear (τ), is governed by $\bar{R}_{22}$, the two-point 'lateral' velocity correlation coefficient, the mean shear and the turbulent intensity.

In Equation (25) the integration over $\vec{y}$ can only be effected when the values of $\tau\sqrt{\overline{u_2^2}}$ are known. Now we can easily see that the greatest values of $\tau\sqrt{\overline{u_2^2}}$ exist in two quite distinct regions of the wall jet at any value of the radius R. These regions are the constant stress region of the boundary layer like flow and the middle of the outer mixing region respectively. On the assumption that the turbulent inner region of the wall jet possesses the same structural similarity as the inner region of a flat plate, channel or pipe flow we have that the mean velocity distribution in this region (known as the 'Law of the Wall') is

$$\frac{\bar{u}}{u_\tau} = \frac{1}{K}\ln\left(\frac{Zu_\tau}{\nu}\right) + A \qquad (26)$$

and
$$\tau \equiv \frac{\partial \bar{u}}{\partial Z} = \frac{u_\tau}{KZ} \tag{27}$$

where $u_\tau = \sqrt{\tau_w/\rho}$ is the shear velocity.

Equation (26) is known to hold for $Zu_\tau/\nu > 30$ and $Z/Z_m < 0.2$, where Z_m is the thickness of the shear layer up to the maximum velocity $\bar{u} = u_m$. K, known as the von Kármán constant, has a value roughly equal to 0.4. Since the motion in this inner region must be described by universal functions of the wall shear stress, τ_w, and the viscosity, the turbulent intensity $\overline{u_Z^2}$ must be proportional to u_τ^2. From the measurements of Laufer[3] in a circular pipe it is found that

$$\frac{\overline{u_Z^2}}{u_\tau^2} = a \tag{28}$$

a constant over most of the inner region. (a is of the order of unity). From Equations (27) and (28) we see that

$$\tau\sqrt{\overline{u_Z^2}} = \frac{a}{K\nu} \frac{u_\tau^3}{(Zu_\tau/\nu)} \tag{29}$$

for values of $(Zu_\tau/\nu) > 30$. Nearer the wall it is found that

$$\tau\sqrt{\overline{u_Z^2}} \approx 0.009 \left(\frac{Zu_\tau}{\nu}\right)^2 \frac{u_\tau^3}{\nu} \tag{30}$$

and it is interesting to note that the maximum value of $\tau\sqrt{\overline{u_Z^2}}$ occurs just outside the laminar sub-layer. In fact it is very close to the region where the total turbulent intensity $(\overline{u_R^2} + \overline{u_\phi^2} + \overline{u_Z^2})$ reaches its maximum value (Fig.1).

It is found from (29), (30) that

$$\int_0^{Z_m} f(Z^*) \frac{dZ^*}{(u_\tau^3/\nu)^2} = 0.43 \tag{31}$$

where $f(Z^*) = \tau^2 \overline{u_Z^2}$ and $Z^* = (Z\, u_\tau/\nu)$. Thus the average value of $\tau^2 \overline{u_Z^2}$ in the region $0 < Z < Z_m$ is $0.43\, u_\tau^5/\nu Z_m$.

On the other hand it is shown in Section 8 that the value of the mean shear in the outer mixing region is

$$\tau = \frac{-0.616\, u_m}{(Z_{1/2} - Z_m)} \tag{32}$$

where $Z_{1/2}$, Z_m are the distances to the points of half and maximum velocity respectively. On the assumption that in this latter region $\sqrt{\overline{u_Z^2}} \sim 0.15\, u_m$ we find that

$$\tau^2 \overline{u_Z^2} = \frac{0.0085\, u_m^4}{(Z_{\frac{1}{2}} - Z_m)^2} \tag{33}$$

This more or less completes the formal treatment of the pressure fluctuations in a wall jet. Since the contributions to $\overline{p^2}$ from the inner region and the outer mixing region are very different in magnitude (see (31) and (33)) we will consider them separately.

3. PRESSURE FLUCTUATIONS DUE TO THE BOUNDARY LAYER TYPE SHEAR FLOW

From (25) we found that

$$P(\vec{x};\ \vec{x}')_{Z=0} = \frac{\rho^2}{\pi^2} \int_{-\infty}^{\infty} dy_1 \int_{0}^{\infty} dy_2 \int_{-\infty}^{\infty} dy_3 \int_{-\infty}^{\infty} dr_1 \int_{-y_2}^{\infty} dr_2 \int_{-\infty}^{\infty} dr_3\, \bar{R}_{22}(\vec{r})$$

$$\tau(\vec{x};\ y_2)\, \tau(\vec{x};\ y_2 + r_2) \sqrt{\overline{u_2^2}}\,(\vec{x};\ y_2) \sqrt{\overline{u_2^2}}\,(\vec{x};\ y_2 + r_2) \tag{34}$$

$$\frac{\partial}{\partial y_1}\left(\frac{1}{|\vec{x} - \vec{y}|}\right) \frac{\partial}{\partial z_1}\left(\frac{1}{|\vec{x}' - \vec{z}|}\right)$$

If the turbulence is assumed isotropic

$$\bar{R}_{jl}(\vec{r}) = \left(f + \frac{rf'}{2}\right)\delta_{jl} - \frac{f'}{2r} r_j\, r_l \tag{35}$$

where f is the longitudinal velocity correlation coefficient and $f' \equiv df/dr$. Hence

$$\bar{R}_{22}(\vec{r}) = f - \frac{rf'}{2} - \frac{f'}{2r} r_2^2 \tag{36}$$

This form for $\bar{R}_{22}$ does not agree too well with the experimental results of Grant[10] and others. However, the errors involved in the use of (35) can be shown to be small.

If we use the result from Appendix B (Eqn. B-12) we find that approximately

$$P(\vec{x},\ o)_{Z=0} = \frac{8a}{15} \rho^2 \langle \tau^2 \overline{u_2^2} \rangle \int_0^{\infty} rf\, dr \tag{37}$$

where a is an anisotropy factor which is assumed to have a value of about 1/3, and from (31)

$$\langle \tau^2 \overline{u_Z^2} \rangle \approx \frac{0.43\, u_\tau^5}{\nu Z_m} \tag{38}$$

If we now insert

$$f = \exp\left(\frac{-r}{l_p}\right) \tag{39}$$

with

$$\int_0^\infty f\, dr = l_p \tag{40}$$

into (37)

$$\frac{\sqrt{P(\vec{x},\ o)_{Z=c}}}{\frac{1}{2}\rho\, u_m^2} \approx 0.28\, \frac{l_p}{Z_m}\sqrt{\frac{Z_m\, u_\tau}{\nu}}\, c_f \approx 3c_f \tag{41}$$

where we have used* $l_p = 0.3\ Z_m$; $Z_m\ u_\tau/\nu = 1600$ and $c_f = \tau_w/\frac{1}{2}\rho\, u_m^2$ is the local skin friction coefficient. This result is similar to that found by Kraichnan[5] for the boundary layer on a flat plate, except that our factor 3 replaces the range 2 to 12 as given by Kraichnan although we note that strictly $\sqrt{P(o)}/\frac{1}{2}\rho\, u_m^2$ is proportional to $c_f^{5/4}$ and $\sqrt{Z_m\ u_m/\nu}$.

Equation (41) can be compared with the results of various experimenters for ordinary boundary layer flow. The measurements of Harrison[7] suggest a value of

$$\sqrt{\overline{p^2}}/\tfrac{1}{2}\rho u_m^2 \approx 0.0095 = 4.8\, c_f \tag{42}$$

while Willmarth[17] gives

$$\sqrt{\overline{p^2}}/\tfrac{1}{2}\rho u_m^2 = 0.006 = 2.5\, c_f \tag{43}$$

Our measurement on the wall of a wind tunnel with a microphone 0.14 in. diameter and a boundary layer displacement thickness of 0.238 in. gave

$$\sqrt{\overline{p^2}}/\tfrac{1}{2}\rho u_m^2 = 0.008 = 3.6\, c_f \tag{44}$$

All these results are qualitatively in fair agreement with the theory and indicate that in a turbulent boundary layer on a flat plate, in zero pressure gradient, the wall pressure fluctuation arises mainly from disturbances in the constant stress region. Since c_f changes only slowly with distance we see that $\sqrt{\overline{p^2}}$ will only change slowly with increase in x.

Finally we should note that our analysis leading to Equation (41) is only approximate. Nevertheless the more accurate analysis given by Lilley[18] leads to a value of $3.1\ c_f$.

---

*This value is obtained from the work of Grant[10] by noting the zero point value of R_{22} (r, 0, 0) in the outer region of a boundary layer

4. PRESSURE FLUCTUATIONS DUE TO THE 'JET MIXING REGION' SHEAR FLOW

In the outer region of the wall jet the structure of the turbulence is largely uninfluenced by the wall. Nevertheless the solution of Equation (6) is still given by (19), for the contribution from the 'image' Green function must still be included. However, the problem is simpler because $\tau^2\overline{u_Z^2}$ is approximately constant over the region centred about the middle of the mixing region at any radius. Equation (25) therefore reduces to

$$P(\vec{x},\ \vec{x}')_{Z=0} = \frac{\rho^2}{\tau^2}\tau^2(\vec{x})\ \overline{u_2^2}(\vec{x}) \int_{-\infty}^{\infty} dy_1 \int_{0}^{\infty} dy_2 \int_{-\infty}^{\infty} dy_3 \int_{-\infty}^{\infty} dr_1 \int_{-y_2}^{\infty} dr_2 \int_{-\infty}^{\infty} dr_3$$

$$\bar{R}_{22}(\vec{r})\frac{\partial}{\partial y_1}\left(\frac{1}{|\vec{x} - \vec{y}|}\right)\frac{\partial}{\partial z_1}\left(\frac{1}{|\vec{x}' - \vec{z}|}\right) \qquad (45)$$

If we again put $(\vec{x}' - \vec{x}) = 0$ then from Appendix B

$$P(\vec{x};\ \vec{x})_{Z=0} \approx \frac{8\alpha}{15}\rho^2\ \tau^2(\vec{x})\ \overline{u_2^2}(\vec{x}) \int_{0}^{\infty} rf\ dr \qquad (46)$$

where α is the anisotropy factor.

If, further, $$f = \exp(-r/l_0) \qquad (47)$$

then $$P(\vec{x};\ \vec{x})_{Z=0} = \frac{8\alpha}{15}\rho^2\ \tau^2\ \overline{u_Z^2}\ l_0^2 \qquad (48)$$

On inserting the values for $\tau^2\ \overline{u_Z^2}$ from (33) and putting*

$$l_0 = (Z_{\frac{1}{2}} - Z_n) \qquad (49)$$

then $$\frac{\sqrt{\overline{p^2}}}{\frac{1}{2}\rho u_\tau^2} \approx 0.1 \qquad (50)$$

The value obtained from our measurements is

$$\frac{\sqrt{\overline{p^2}}}{\frac{1}{2}\rho u_\tau^2} = 0.11 \qquad (51)$$

and indicates that the contribution to $\sqrt{\overline{p^2}}$ from the outer mixing region is some ten times that from the inner boundary layer like flow. This result is not surprising

*This value of l_0 corresponds to the half-width of the outer mixing region. At first sight this value seems unduly high but it is in keeping with the results of the large eddy analysis in Appendix C and the measured spectra.

when one remembers that the small shear in the outer mixing region is acting over a distance many times that of the entire inner boundary layer thickness.

The theoretical value of $\sqrt{\overline{p^2}}/\frac{1}{2}\rho u_m^2$ is independent of the radius (R) and this is confirmed by our experimental results. This altogether interesting result is we feel most important, for it shows that even in a region of flow where the velocity changes in the mainstream direction are large ($u_m \sim 1/R$), the pressure fluctuations are still largely determined by local conditions only. This agrees with the results of the mean shear stress on the wall by Bradshaw and Love[13] (Fig.2). They showed that the skin friction coefficient, although slightly higher than for a flat plate, changed very slowly with increase in radius beyond an inner radius where the wall jet was being established.

5. THE SPECTRUM AND SPACE PRESSURE CORRELATION FOR ZERO TIME DELAY

In Sections (3) and (4) the formal treatment of the pressure covariance with zero time delay is given, but only the results for the mean square of the pressure are evaluated in full. However, Lilley[19] has already evaluated the pressure covariance in free shear flow turbulence, and as we have seen above the results for wall turbulence will be similar apart from a numerical factor. From Lilley's results for $P(\vec{x};\ \vec{x}')$ with $f = \exp(-\sigma^2 r^2)$, we find (Fig.3) that $P(\vec{x};\ \xi_1,\ 0,\ 0)$ has a large negative loop with a zero crossing point of $\sigma\xi_1 \approx 1$. On the other hand $P(\vec{x};\ 0,\ 0,\ \xi_3)$ is positive for all values of ξ_3 and falls to zero as $\xi_3 \to \infty$ much more slowly than $f(r)$, as $r \to \infty$. This isotropic turbulence model used in evaluating these results is a little too crude to make comparison with experiment justified, apart from an order of magnitude basis, yet it is interesting to note that Harrison[7] found similarly positive values for $P(\vec{x};\ 0,\ 0,\ \xi_3)$, although the fall-off at large values of ξ_3 was slower than in our results. However, this is what one might expect from the anisotropy in the large scale turbulence modifying the form of $\bar{R}_{22}(\vec{r})$ at large values of $|\vec{r}|$.

The wall pressure spectrum function has been evaluated in Appendix C taking into account the large eddy structure, and in Appendix E allowing for convection. In both these cases and also in the free shear flow turbulence example, the spectrum at low frequencies obeys the law $\bar{\omega}^2.\exp(-\bar{\omega}^2)$ - (Fig.4). In our wall jet experiments we find such a rise at low frequencies, in contrast with all measurements made in pipes and on tunnel wall boundary layers, where the flatness of the moderately low frequency end of the spectrum is marked.

Harrison[7] has also remarked on this flatness of the spectra at low frequencies and has suggested that, except at the very lowest frequencies outside the range of the measuring equipment, this might be explained in terms of the intermittency of the boundary layer. However, this does not in itself explain the relatively high energy content in the lower frequencies.

A complete explanation of this phenomenon has not yet been found, assuming of course that the flatness in the low frequency end of the spectra is not associated with spurious wind tunnel effects, such as fan noise, flow noise extra and above the boundary layer noise, or tunnel circuit resonance. However, a clue to the explanation may come from an analysis of results similar to the space-time correlations of wall pressure

obtained by Willmarth[6]*. These data show, as explained in Appendix D, that the spatial pressure correlation for optimum time delay (i.e. roughly the autocorrelation in axes moving with the mean convection speed of the eddies) does not fall to negative values at large separation distances in contrast to the autocorrelation measured in axes fixed in the wall. This means that the life times of the big eddies are being extended on account of the growing scale associated with the slow increase in the boundary layer thickness. This consequent modification of the autocorrelation in moving axes at large times could produce some lift to the low frequency end of the spectra although a fall off like $\bar{\omega}^2$ might still be expected at the very lowest frequencies.

On the other hand it would appear that in the case of the wall jet, since the increase in shear layer thickness is relatively large coupled with the rapid fall off in velocity with increase in radius, the life time of the eddy could not be extended in this way. These differences between the theoretical and experimental spectra for both the wall jet and boundary layer are being further investigated.

6. THE WALL JET - THEORY OF THE MEAN FLOW

The wall jet has been studied theoretically by Glauert[11] and experimentally by Bakke[12] and Bradshaw[3]. Although Glauert found solutions for both the laminar and turbulent problems only the turbulent case will be required here. He found that the velocity distribution in the vicinity of the wall was similar to that in a boundary layer with zero pressure gradient. In the inner region one would expect the 'law of the wall' to apply but for simplicity Glauert assumed the Blasius distribution

$$\frac{\bar{u}_R^2}{u_\tau^2} = \left(\frac{\bar{u}_R\, Z}{\nu}\right)^{1/4} \Big/ \; 0.0225 \qquad (52)$$

where u_τ is the shear velocity given by $u_\tau = \sqrt{(\tau_w/\rho)}$.

In the outer region Glauert evaluated the velocity distribution numerically and showed that it is slightly fuller than that given by a (1/7)th power law. The maximum velocity occurs at $Z/Z_{\frac{1}{2}} = 0.125$, for a value of $(u_m/\nu)(Z_{\frac{1}{2}} - Z_m) = 4 \times 10^4$, where $Z_{\frac{1}{2}}$ is the ordinate to the point in the outer mixing region for which $\bar{u}_R/u_m = 0.5$. The value $Z/Z_{\frac{1}{2}} = 0.125$, where $u = u_m$, differs from that obtained experimentally by Bakke, but this can be explained from Glauert's analysis, for Bakke's value of $(u_m/\nu)(Z_{\frac{1}{2}} - Z_m) = 3.5 \times 10^3$, compared with our value above of 4×10^4.

The distribution of maximum velocity with radial distance follows the law

$$\bar{u}_R \sim \frac{1}{R^{1.05}} \qquad (53)$$

at the Reynolds numbers of the tests reported here.

---

*Results analogous to these have been obtained by Favre and his co-workers[20] for the two-point velocity correlations with separation in the streamwise direction.

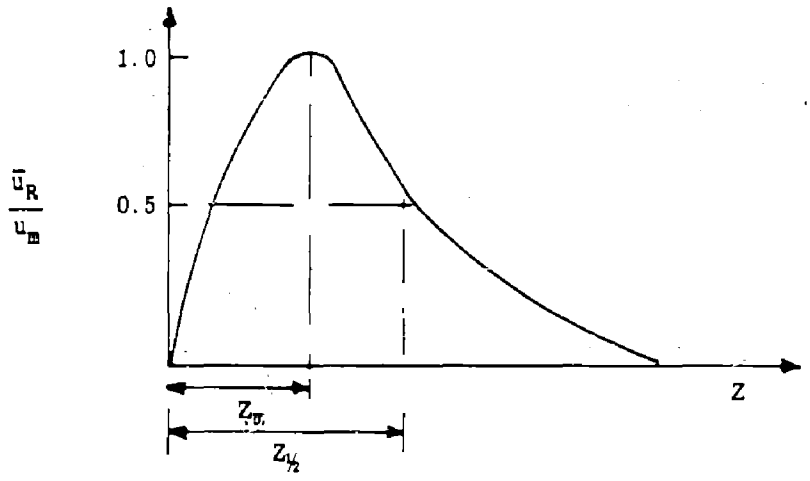

The velocity distribution in the outer mixing region is found by Glauert to be given approximately by

$$\frac{\bar{u}_R}{u_m} = \operatorname{sech}^2\left\{0.875\left(\frac{Z - Z_m}{Z_{1/2} - Z_m}\right)\right\} \qquad (54)$$

where $Z_{1/2} \sim R^{0.9}$.

The experiments of Bakke confirm these predictions. Bradshaw and Love give some results for the variation of wall shear stress under the wall jet. These show that in the region of fully developed flow the wall shear stress is some 25% higher than in the corresponding case (i.e. equal u_m and Z_m) for the flow over a flat plate in zero pressure gradient.

7. APPARATUS

Wall-Jet

The test rig shown in Figure 5 was geometrically similar to that used by Bakke[12] for confirmation of the theoretical results obtained by Glauert[11]. The jet was 1.5 inches diameter and air was supplied from pressurised reservoir tanks via a 6 inch diameter throttling valve and 200 feet of 6 inch diameter pipe, part of the laboratory ring-main supply which passes horizontally 18 feet above the test site. The vertical downpipe was 3 inches diameter and 10 feet long connected to the 6 inch main through a 3 inch isolating valve. This was followed by a smooth contraction containing a wire gauze and then 5 feet of 1.5 inch diameter smooth-bore pipe fitted with a 6 inch diameter flange forming the jet. The jet flange was 0.75 inch above the plate.

Two plates, each measuring 4 feet square, were used. One was constructed of light acoustic boarding 2 inches thick lined with thin Bakelite sheet; the other was of 2 inch thick Tufnol about 100 lb in weight.

The test procedure was to open the 3 inch valve fully and to control the air-flow by the main 6 inch valve at the reservoir tanks. This was necessary to keep the valve and pipe noise to a minimum.

The measuring region was 3-10 jet diameters from the jet axis over which the jet half width (distance to half-maximum velocity) varied from 0.4 inch to 1.2 inches with maximum velocities of 140 f/s to 40 f/s.

Pressure Transducers

Ammonium di-hydrogen phosphate crystal transducers, type M213 and M141, were used. These are manufactured by the American Massa Company.

The M213 has an outside diameter of 0.22 inch and a diaphragm diameter of 0.14 inch. Its capacity is 12 pf and has a level frequency response to 120 kc/s. It is used with a low noise and low microphone cathode-follower connected through 6 inches of low-noise cable. The input impedance of the cathode-follower is 200 megohms shunted by 6 pf, allowing a response down to 20 c/s. The cathode-follower noise level is 5 μV, although below 300 c/s the noise from the transducer is 25 μV. A high-pass filter with a cut-off at 250 c/s can be inserted, but is not normally necessary. The sensitivity at the cathode-follower in the output terminals is -111 decibels re 1 volt/microbar (approximately 2.8 microvolt/(dyne/cm^2)).

The signal was amplified by a battery powered low-noise amplifier of 28 decibels voltage gain, followed by an amplifier of 94 decibels voltage gain. Root mean square readings were measured on a meter of the linear averaging type. The bandwidth of the amplifiers was 5 c/s to above 500 kc/s.

The M141 has a diameter of 0.6 inch, a capacity of 110 pf and a sensitivity at the cathode-follower output terminals of -94 decibels re 1 volt/microbar (approximately 20 microvolts/(dyne/cm^2)). The low frequency noise of this transducer is much lower than that of the M213 due to its higher capacitance, and the usable frequency response is 20 c/s - 30 kc/s.

The transducers were mounted in the light acoustic-board plate in soft rubber sleeves and in the Tufnol plate with a heavy brass body and 'O' ring suspension, similar to that of Willmarth[17]. The use of the two methods of fixing in the two very different plates was to ensure that the measurements were not affected by the vibration of the transducers due to the impingement of the jet on the plate.

Spectrum measurements were made using a set of third octave filters, covering the range 40 c/s - 20 kc/s.

Correlator

The correlator used in the space and time correlations of pressure and velocity fluctuations worked on the analogue principle. The multiplier was of the quarter-squaring type and used two special squaring valves. The design was based on that of Miller, Soltes and Scott[21]. However, much improved circuitry was employed so that, if necessary, multiplication could be accomplished over the bandwidth DC - 200 kc/s. The accuracy was not of the standard associated with computing multipliers, but is of the order of 1 - 2% which is quite acceptable for the present purpose. The output was read on a DC galvanometer with a time constant variable between 2 - 10 seconds.

A time delay is accomplished on a twin channel tape recorder of extremely low wow and flutter, using one fixed and one moving head. The recorder used 0.5 inch wide tape running at 75 inch/second.

The two signals to be correlated were first recorded on a loop of tape giving a sample length of 2 seconds (this sample length could be increased if extra idling pulleys were fitted to the machine) and then played back inserting the required time delay by manual control of the moving head. The signals could either be recorded on a frequency modulation system bandwidth DC - 20 kc/s or on an amplitude modulation system with a bandwidth of 250 c/s - 100 kc/s. The signal to noise ratio was 42 decibels.

The correlator was capable of correlating a 100 kc/s sine-wave with 15 points to the period. The maximum time delay possible was 40 millisecs and the minimum increment was 0.67 microseconds.

8. PRELIMINARY RESULTS AND DISCUSSION

The measurements of mean velocity across the wall jet from 3 to 10 diameters from the jet axis showed good agreement with the similarity profiles obtained theoretically by Glauert[11] and experimentally by Bakke[12] (Figs.6 and 7). The maximum velocity varied as $R^{-1.05}$, where R is the distance from the jet axis, and the jet half thickness $Z_{\frac{1}{2}}$ varied as $R^{0.9}$. The maximum velocity occurred at $Z/Z_{\frac{1}{2}} = 0.15$ corresponding to a Reynolds number $u_m(Z_{\frac{1}{2}} - Z_m)/\nu = 2 \times 10^4$.

The measurements of the wall pressure fluctuations from 3 to 10 diameters from the jet axis showed that

$$\sqrt{\overline{p^2}}/\tfrac{1}{2}\rho u_m^2 = 0.11$$

and was approximately independent of radius (Fig.8). The corresponding spectra (Fig.9) obeyed a similarity law on the basis of the frequency parameter $\omega(Z_{\frac{1}{2}} - Z_m)/u_m$. A typical autocorrelation is shown in Figure 10.

Comparative results were also obtained in the College of Aeronautics 20 in. × 11 in. low-turbulence wind tunnel at a position in the working section where the displacement thickness was 0.286 in. at a freestream speed of 126 f/s. The corresponding value of the skin friction coefficient, c_f, obtained from the measured velocity profile, was 0.0022. The value of $\sqrt{\overline{p^2}}/\tfrac{1}{2}\rho u_m^2$ was 0.008 which is in fair agreement with the measurements of Willmarth and Harrison. However, this result cannot be relied upon quantitatively because in this tunnel the low frequency extraneous noise level is not low, although inevitably its contribution to the total pressure energy is small. Perhaps what is more important is that it provides a check both on the accuracy of the instrumentation used, and on the values of $\sqrt{\overline{p^2}}/\tfrac{1}{2}\rho u_m^2$ as found in the wall jet using the same pressure transducers.

The large values of $\sqrt{\overline{p^2}}/\tfrac{1}{2}\rho u_m^2$ as measured on the wall jet are not special to that case and have been found by Owen[22] to exist on wings in regions of separated flow. However, the experimental data on the effect of pressure gradient on wing pressure fluctuations are so few that we can only speculate that, on the basis of our theory, the surface pressure fluctuations will be high when either the value of c_f is high, say at transition, or the mean shear layer is very thick, say approaching and beyond separation.

9. CONCLUSIONS

A review of theoretical and experimental work on wall pressure fluctuations in turbulent boundary layers has been presented. The theory due to Kraichnan is modified and extended to include the separate effects of the large eddy structure and the convection of the eddies, and the treatment covers both the turbulent boundary layer on a flat plate and the wall jet. The latter case is presented for it provides data in the important practical case when the turbulence is being subjected to a rapid variation in mean shear, not unlike that associated with the flow approaching and beyond separation.

Preliminary theoretical and experimental data for the wall jet give values of $\sqrt{p^2}/\frac{1}{2}\rho u_m^2$ many times that of corresponding measurements on a flat plate with zero pressure gradient. These results are explained in terms of the greater thickness of the shear layer, the relatively high intensity of the turbulence, and the presence of relatively large eddies in the flow.

The present work is intended as a basis for further work at both low speeds and in the more important practical areas of supersonic and hypersonic flight.

REFERENCES

1. Heisenberg, W. — *Zur Statistischen Theorie der Turbulenz.* Z. Phys, 124, 1948, p. 628.

2. Obukhoff, A.M. — *Pressure Pulsations in a Turbulent Flow.* Ministry of Supply, England. Translation P 21452 T, 1949.

3. Batchelor, G.K. — *Pressure Fluctuations in Isotropic Turbulence.* Proc. Cam. Phil. Soc., 47, Part 2, 1951, p. 359.

4. Kraichnan, R.H. — *Pressure Field within Homogeneous Anisotropic Turbulence.* J. Acoust. Soc. Amer., 28, 1956, p. 64.

5. Kraichnan, R.H. — *Pressure Fluctuations in Turbulent Flow over a Flat Plate.* J. Acoust. Soc. Amer. 28, 1956, p. 378.

6. Willmarth, W.W. — *Space-Time Correlations and Spectra of Wall Pressure in a Turbulent Boundary Layer.* NASA Memo 3-17-59W, 1959.

7. Harrison, M. — *Pressure Fluctuations on the Wall Adjacent to a Turbulent Boundary Layer.* Hydromechanics Laboratory Report 1260, David Taylor Model Basin, 1958.

8. Townsend, A.A. — *The Structure of Turbulent Shear Flow.* Cambridge University Press, 1956.

9. Laufer, J. — *The Structure of Turbulence in Fully Developed Pipe Flow.* NACA Report 1174, 1955.

10. Grant, H.L. — *The Large Eddies of Turbulent Motion.* Jn. Fluid Mech., Vol. 4, Part 2, June 1958, p. 149.

11. Glauert, M.B. — *The Wall Jet.* Jn. Fluid Mech. 1, Part 6, 1956, p. 625.

12. Bakke, P. — *An Experimental Investigation of a Wall-Jet.* Jn. Fluid Mech. 2, Part 5, 1957.

13. Bradshaw, P. Love, E.M. — *The Normal Impingement of a Circular Air Jet on a Flat Surface.* A.R.C. 21, 268, Sept. 1959.

14. Curle, N. — *The Influence of Solid Boundaries upon Aerodynamic Sound.* Proc. Roy. Soc. A, 231, 1955, p. 505.

15. Phillips, O.M. — *Surface Noise from a Plane Turbulent Boundary Layer.* Proc. Roy. Soc. A. 234, 1956, p.327.

16. Doak, P.E. — *Acoustic Radiation from a Turbulent Fluid Containing Foreign Bodies.* Proc. Roy. Soc. A. 254, 1960, p.129.

17. Willmarth, W.W. — *Wall Pressure Fluctuations in a Turbulent Boundary Layer.* NACA TN 4139, 1958.

18. Lilley, G.M. — *Pressure Fluctuations in an Incompressible Boundary Layer.* C. of A. Report 133, 1960.

19. Lilley, G.M. — *On the Noise from Air Jets.* ARC 20,376 Unpublished, 1958.

20. Favre, A. — *Quelques Résultats d'Expériences sur la Turbulence ~~Co~~rrélations Spatio-Temporelles Spectres.* Publications Scientifiques et Techniques du Ministère de l'Air, No.N.T.73. 1958.

21. Miller, J.A. et alii — *Wide-Band Analog Function Multiplier.* Electronics, Feb. 1955, p. 160.

22. Owen, T.B. — *Techniques of Pressure Fluctuation Measurements Employed in the RAE Low Speed Wind Tunnels.* AGARD Report 172, 1958.

23. Feynman, R.P. — Phys. Rev. 76, 1949, p. 769.

24. Townsend, A.A. — *The Turbulent Boundary Layer.* Boundary Layer Research Symposium, Freiburg, August 1957.

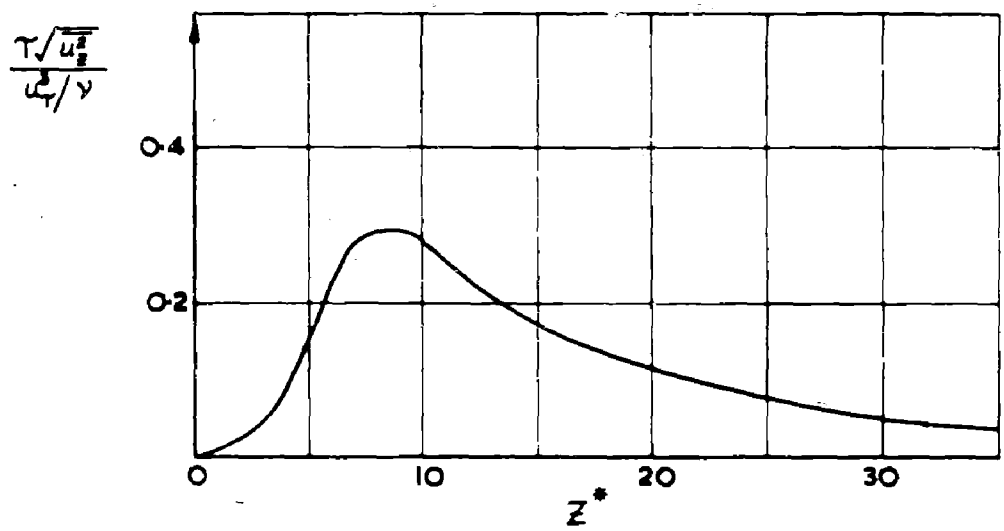

Fig.1 Distribution of the product of mean shear and turbulent intensity in a boundary layer close to the wall

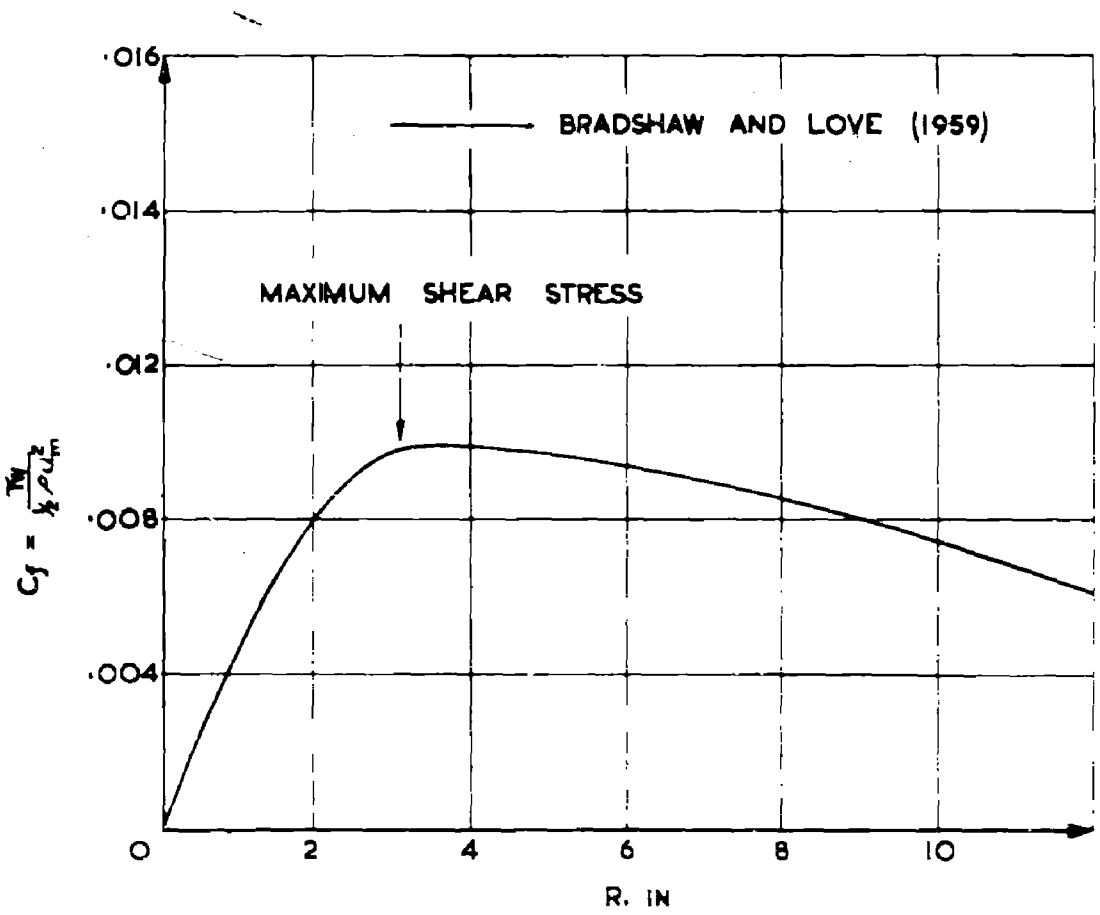

Fig.2 Variation of the skin friction coefficient with radius for the wall jet

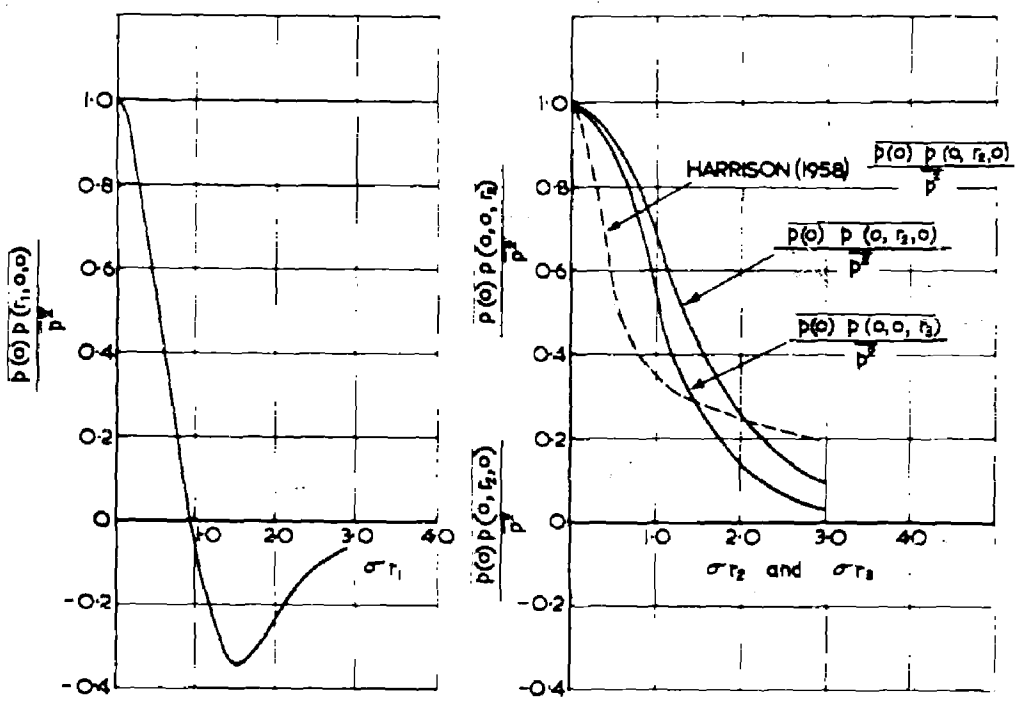

Fig.3 Pressure correlations in isotropic turbulence superposed on mean shear (τ_{12})
$f(r) = \exp(-\sigma^2 r^2)$

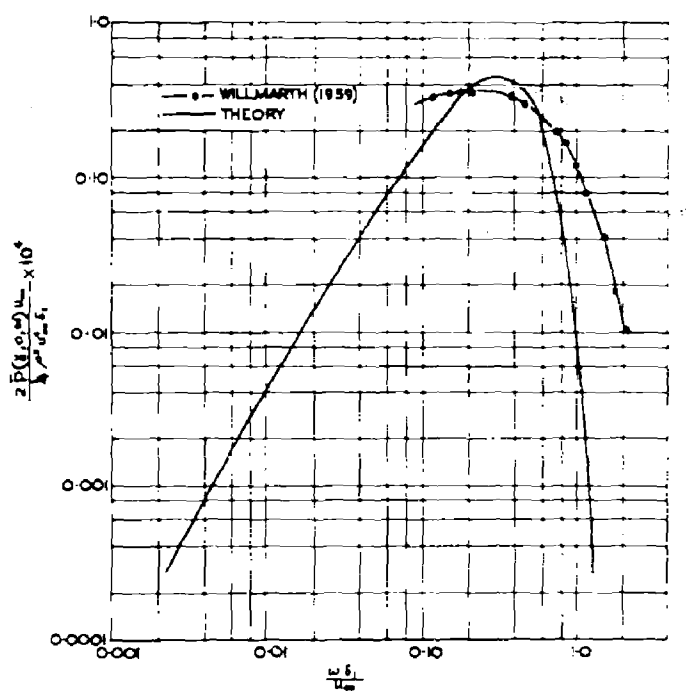

Fig.4 Comparison between measured and theoretical pressure spectrum for a boundary layer

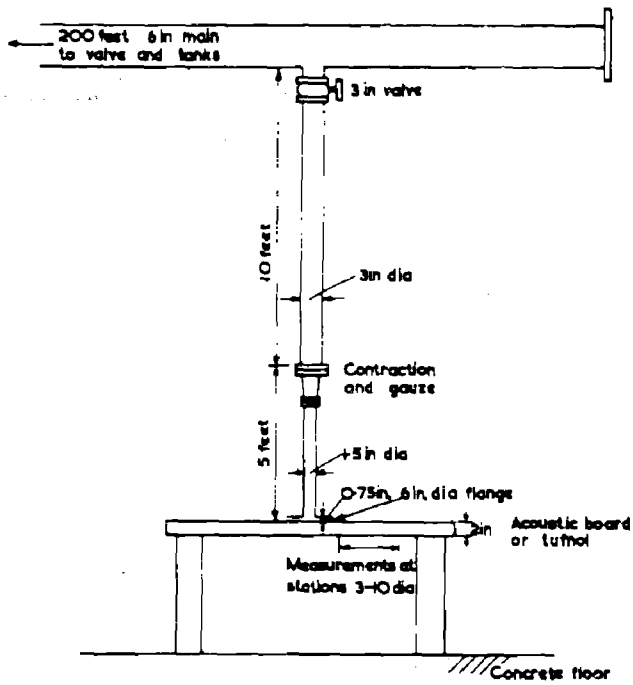

Fig.5 Wall jet configuration

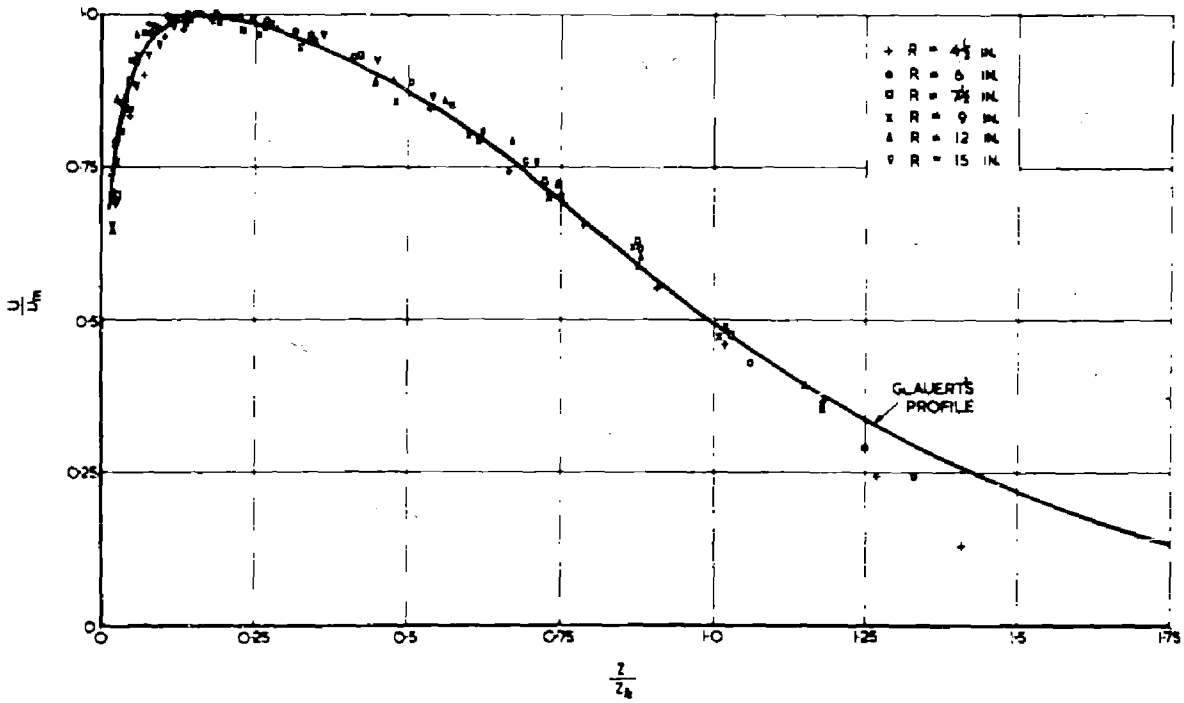

Fig.6 Wall jet mean velocity profiles. $\frac{u_m(Z_{1/2}-Z_m)}{\nu} = 2 \times 10^4$, $\frac{Z_m}{Z_{1/2}} = 0.15$

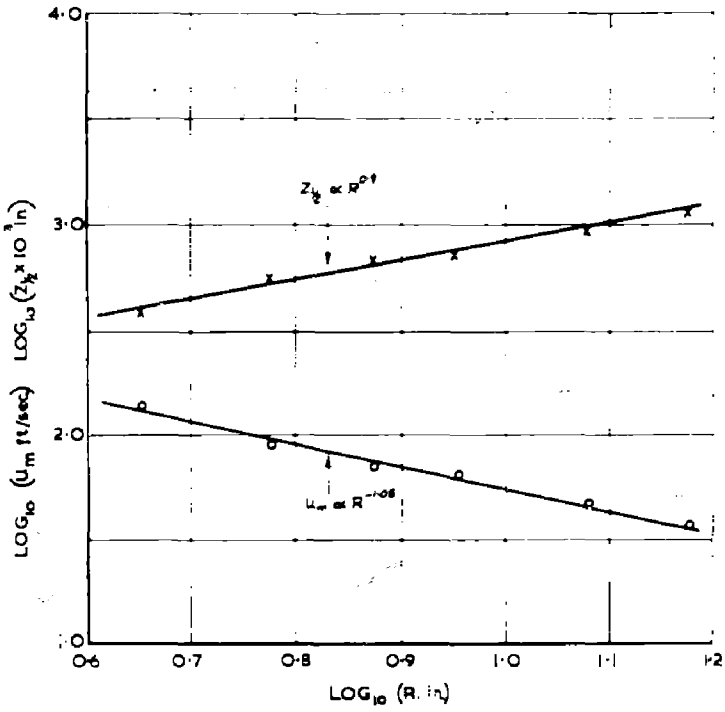

Fig.7 Variation of width of jet $Z_{\frac{1}{2}}$ and maximum velocity u_m with radius R

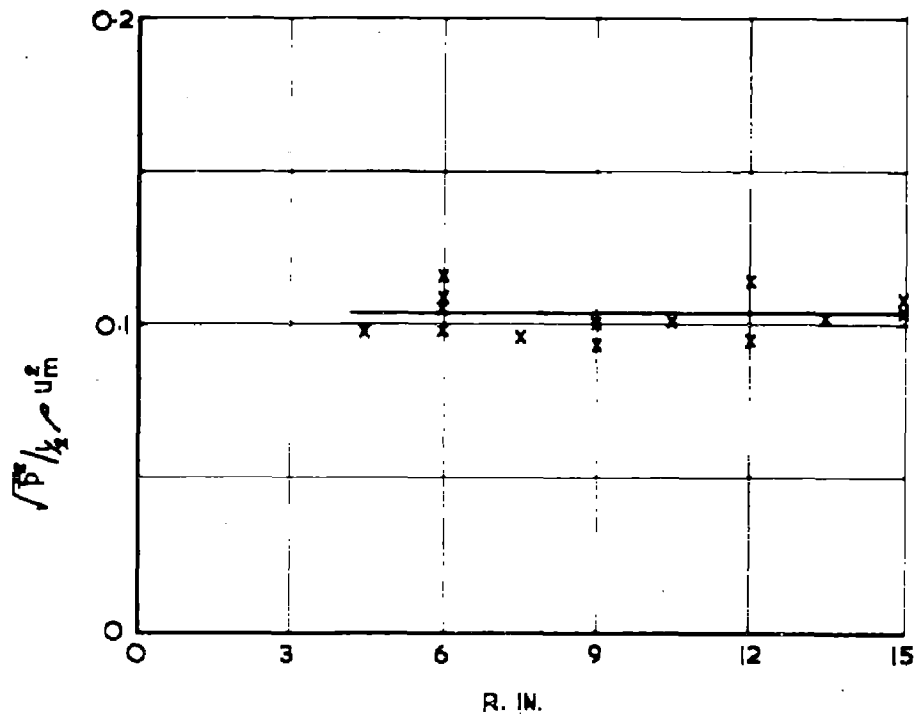

Fig.8 Variation of $\sqrt{\overline{p^2}}/\frac{1}{2}\rho u_m^2$ with radius R

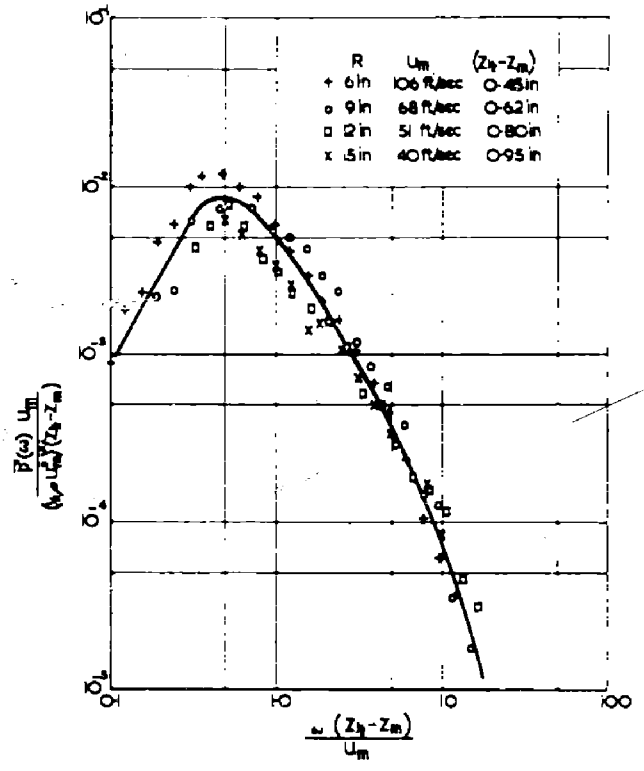

Fig.9 Power spectra of wall jet pressure fluctuations

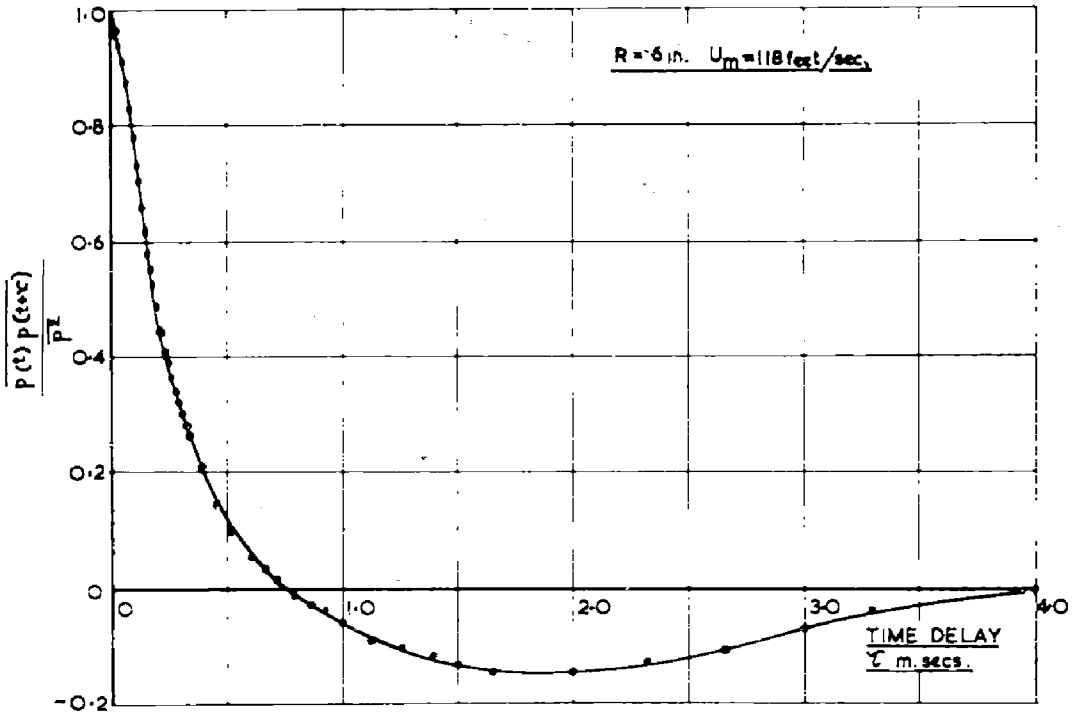

Fig.10 Wall jet autocorrelation of pressure fluctuations

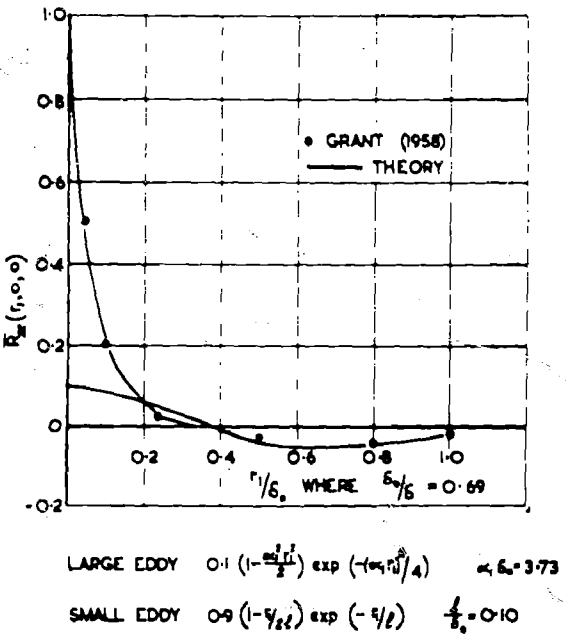

Fig. 11 Comparison between theory and experiment for $\bar{R}_{22}(r_1, 0, 0)$ in a turbulent boundary layer $y/\delta_0 = 0.076$

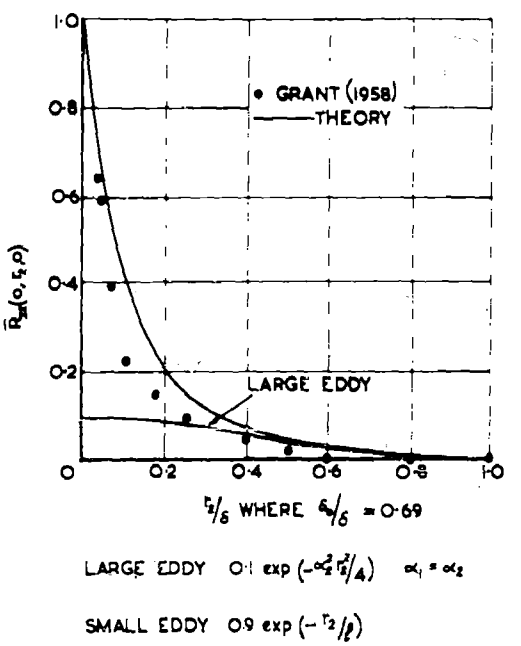

Fig. 12 Comparison between theory and experiment for $\bar{R}_{22}(0, r_2, 0)$ in a turbulent boundary layer $y/\delta_0 = 0.059$

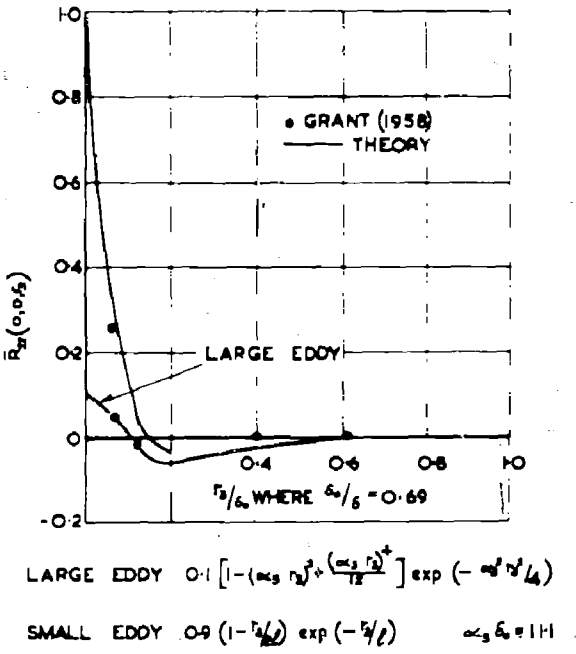

Fig. 13 Comparison between theory and experiment for $\bar{R}_{22}(0,0,r_3)$ in a turbulent boundary layer $y/\delta_c = 0.052$

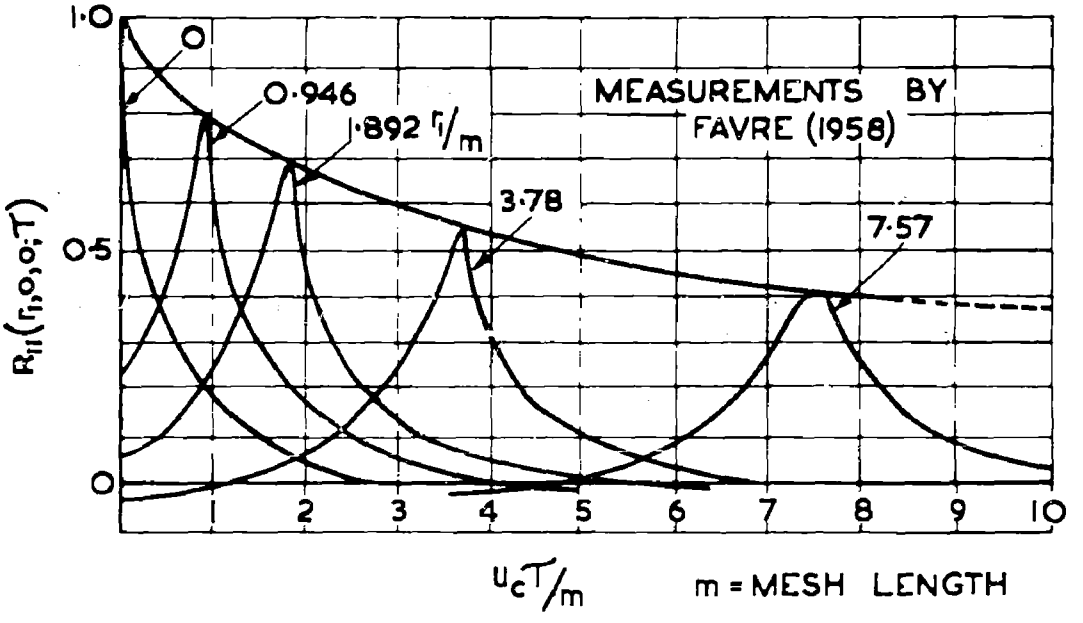

Fig. 14 Comparison between autocorrelations of $\bar{R}_{11}(r_1,0,0;\tau)$ in the fixed and moving frames in grid turbulence

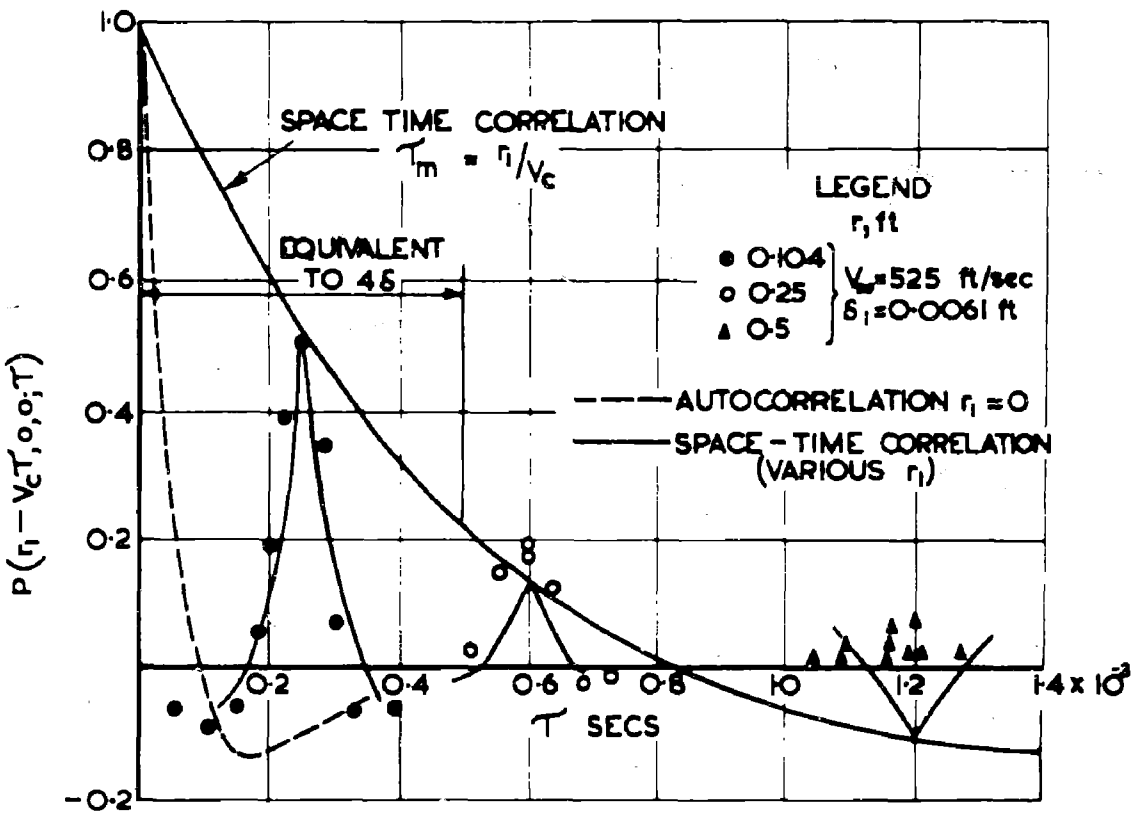

$$P(r_1 - V_c\tau, r, o, o; \tau) = (1-\sigma(r_1 - V_c\tau))(1-\nu|\tau|)\exp(-\sigma|r_1 - V_c\tau|)\exp(-\nu|\tau|)$$

WITH $\nu = \sigma V'$ $\quad V_c = 0{\cdot}8\,V_\infty$ $\quad 1/\sigma = 0{\cdot}033$ ft $\quad V'/V_c \approx 1/10$

Fig. 15 Boundary layer wall pressure fluctuations space-time correlation - Comparison between theory and experiment

APPENDIX A

The Pressure Equation for the Wall Jet

The equations of continuity and motion for an incompressible flow are, in vector notation:

$$\nabla\cdot(\vec{u}) = 0 \tag{A-1}$$

$$\frac{\rho D\vec{u}}{Dt} = -\nabla p + \mu\nabla^2\vec{u} \tag{A-2}$$

where

$$\frac{D}{DT} \equiv \frac{\partial}{\partial t} + (\vec{u}\cdot\nabla) \tag{A-3}$$

If in the cylindrical co-ordinate system (R, ϕ, Z) we write the corresponding velocity components (u_R, u_ϕ, u_Z), then the pressure distribution equation, found from subtracting the time derivative of (A-1) from the divergence of (A-2),

$$\nabla^2 p = -\rho\,\nabla\cdot(\vec{u}\cdot\nabla)\,\vec{u} \tag{A-4}$$

can be written in full as

$$-\frac{\nabla^2 p}{\rho} = \frac{1}{R}\frac{\partial}{\partial R}R\left(u_R\frac{\partial u_R}{\partial R} + \frac{u_\phi}{R}\frac{\partial u_R}{\partial \phi} + u_Z\frac{\partial u_R}{\partial Z} - \frac{u_\phi^2}{R}\right)$$

$$+\frac{1}{R}\frac{\partial}{\partial \phi}\left(u_R\frac{\partial u_\phi}{\partial R} + \frac{u_\phi}{R}\frac{\partial u_\phi}{\partial \phi} + u_Z\frac{\partial u_\phi}{\partial Z} + \frac{u_R u_\phi}{R}\right)$$

$$+\frac{\partial}{\partial Z}\left(u_R\frac{\partial u_Z}{\partial R} + \frac{u_\phi}{R}\frac{\partial u_Z}{\partial \phi} + u_Z\frac{\partial u_Z}{\partial Z}\right) \tag{A-5}$$

Now the mean velocity $\vec{\bar{u}} = (\bar{u}_R,\ 0,\ \bar{u}_Z)$ satisfies the continuity equation

$$\frac{1}{R}\frac{\partial}{\partial R}(R\,\bar{u}_R) + \frac{\partial}{\partial Z}\bar{u}_Z = 0 \tag{A-6}$$

(with Z measured normal to the plane), so that if we write R, $\bar{u}_R$ as a dimension and velocity of order unity, O(1), then Z, $\bar{u}_Z$ are each O(δ) where δ is the thickness of the shear layer. Since terms involving squares and products of fluctuating quantities will be small compared with those involving products of fluctuating quantities and mean flow derivatives, the only terms of importance in (A-5) are for $R \gg 0$,

$$-\frac{\nabla^2 p}{\rho} = \frac{1}{R}\frac{\partial}{\partial R} R\left(u_R \frac{\partial \bar{u}_R}{\partial R} + u_Z \frac{\partial \bar{u}_R}{\partial Z}\right)$$

$$+\frac{\partial}{\partial Z}\left(\bar{u}_R \frac{\partial u_Z}{\partial R} + u_Z \frac{\partial \bar{u}_Z}{\partial Z}\right)$$

$$\pm \frac{\partial u_R}{\partial R}\frac{\partial \bar{u}_R}{\partial R} + 2\frac{\partial u_Z}{\partial R}\frac{\partial \bar{u}_R}{\partial Z} + \frac{\partial u_Z}{\partial Z}\frac{\partial \bar{u}_Z}{\partial Z}$$

$$\doteq 2\frac{\partial u_Z}{\partial R}\frac{\partial \bar{u}_R}{\partial Z} \qquad \text{(A-7)}$$

if mean velocity derivatives of O(1) are neglected.

APPENDIX B

The Evaluation of an Integral

It was shown in Section 2 that the pressure correlation depends on the value of

$$I = \int_{-\infty}^{\infty} dy_1 \int_{0}^{\infty} dy_2 \int_{-\infty}^{\infty} dy_3 \int_{-\infty}^{\infty} dr_1 \int_{-y_2}^{\infty} dr_2 \int_{-\infty}^{\infty} dr_3 \, \bar{R}_{22}(\vec{r}) \, g(y_2) \frac{\partial}{\partial y_1}\left(\frac{1}{|\vec{x} - \vec{y}|}\right)$$

$$\frac{\partial}{\partial z_1}\left(\frac{1}{|\vec{x}' - \vec{z}|}\right) \qquad \text{(B-1)}$$

where $\vec{r} = \vec{z} - \vec{y}$.

Kraichnan[4] has evaluated a similar integral following the method of Feynman[23]. He found that

$$I_{\alpha\beta} = \int_{v} \frac{\partial}{\partial y_\alpha} |\vec{y} - \vec{x}|^{-1} \frac{\partial}{\partial r_\beta} |\vec{y} + \vec{r} - \vec{x}'|^{-1} \, d\vec{y}$$

$$= 2\pi \frac{\partial^2}{\partial r_\alpha \partial r_\beta} |\vec{r} - \vec{\xi}| \qquad \text{(B-2)}$$

where $\vec{\xi} = \vec{x}' - \vec{x}$ and v, the volume of integration, extends to infinity.

If in (B-1) we put

$$\vec{\xi} = \vec{x}' - \vec{x}; \quad \vec{\eta} = \vec{y} - \vec{x}'; \quad \vec{\zeta} = \vec{\eta} + \vec{\xi}; \quad \vec{t} = \vec{\xi} - \vec{r}$$

then with $\vec{\xi}(\xi_1, 0, \xi_3)$

$$I = -\frac{\partial}{\partial \xi_1} \int_{0}^{\infty} g(y_2) \, dy_2 \int_{-y_2}^{\infty} dr_2 \int_{-\infty}^{\infty} dr_1 \int_{-\infty}^{\infty} dr_3 \, \bar{R}_{22}(\vec{r}) \frac{\partial}{\partial t_1} \int_{-\infty}^{\infty} d\zeta_1 \int_{-\infty}^{\infty} d\zeta_3 \times$$

$$\times \frac{1}{\zeta |\vec{\zeta} - \vec{t}_1|} \qquad \text{(B-3)}$$

Let

$$I_1 = \int_{-\infty}^{\infty} d\zeta_1 \int_{-\infty}^{\infty} d\zeta_3 \frac{1}{\zeta |\vec{\zeta} - \vec{t}|} \qquad \text{(B-4)}$$

and if following Feynman we introduce a new variable

$$\vec{\zeta}' = \vec{\zeta} - \frac{\vec{t}}{1+\tau^2} \tag{B-5}$$

and following Kraichnan[4] we use the identity

$$\frac{1}{|a|\cdot|b|} = \frac{2}{\pi}\int_0^\infty \frac{d\tau}{a^2 + b^2\tau^2} \tag{B-6}$$

then
$$I_1 = \frac{2}{\pi}\int_0^\infty \frac{d\tau}{1+\tau^2}\int_{-\infty}^{\infty} d\zeta_1'\int_{-\infty}^{\infty} d\zeta_3' \frac{1}{\zeta'^2 + \frac{t^2\tau^2}{(1+\tau^2)^2}} \tag{B-7}$$

and
$$\frac{\partial I_1}{\partial t_1} = -\frac{4t_1}{\pi}\int_0^\infty \frac{\tau^2\,d\tau}{(1+\tau^2)^3}\int_{-\infty}^{\infty} d\zeta_1'\int_{-\infty}^{\infty} d\zeta_3'\left(\zeta'^2 + \frac{t^2\tau^2}{(1+\tau^2)^2}\right)^{-1} \tag{B-8}$$

$$= -4t'\int_0^\infty \frac{\tau^2 d\tau}{(1+\tau^2)\{\zeta_2'^2(1+\tau^2)^2 + t^2\tau^2\}} \tag{B-9}$$

But because $\xi_2 = 0$ we see that $\zeta_2 = y_2$ and so from (B-3), (B-5) and (B-9)

$$I = 4\frac{\partial}{\partial \xi_1}\int_0^\infty g(y_2)\,dy_2\int_{-y_2}^{\infty} dr_2\int_{-\infty}^{\infty} dr_1\int_{-\infty}^{\infty} dr_3\,\bar{R}_{22}(\vec{r})\,t_1\,\times$$

$$\times\int_0^\infty \frac{\tau^2 d\tau}{(1+\tau^2)\{(y_2(1+\tau^2)+r_2)^2 + t^2\tau^2\}} \tag{B-10}$$

Now the orders of integration with respect to r_2 and y_2 can be reversed

$$\int_0^\infty dy_2\int_{-y_2}^{\infty} dr_2 = \int_0^\infty dr_2\int_0^\infty dy_2 + \int_{-\infty}^{0} dr_2\int_{-r_2}^{\infty} dy_2$$

and hence if
$$\bar{R}_{22}(\vec{r}) \equiv \bar{R}_{22}(r_1, -r_2, r_3)$$

equation (B-10) becomes

$$I = 4\frac{\partial}{\partial \xi_1}\int_{-\infty}^{\infty} dr_1 \int_{0}^{\infty} dr_2 \int_{-\infty}^{\infty} dr_3\, \bar{R}_{22}(\vec{r})\, t_1 \int_{0}^{\infty} \frac{\tau^2 d\tau}{(1+\tau^2)} \times$$

$$\times \left\{ \int_{0}^{\infty} \frac{g(y_2)\, dy_2}{[\{y_2(1+\tau^2) + r_2\}^2 + t^2\tau^2]} + \int_{r_2}^{\infty} \frac{g(y_2)\, dy_2}{[\{y_2(1+\tau^2) - r_2\}^2 + t^2\tau^2]} \right\} \qquad \text{(B-11)}$$

When $g(y_2)$ is a constant, $\bar{g}$, we find after integration with respect to y_2 and τ that

$$I \approx \pi\bar{g} \int_{-\infty}^{\infty} dr_1 \int_{0}^{\infty} dr_2 \int_{-\infty}^{\infty} dr_3\, \bar{R}_{22}(\vec{r}) \frac{\partial}{\partial \xi_1}\left(\frac{\xi_1 - r_1}{|\vec{\xi} - \vec{r}|}\right) \qquad \text{(B-12)}$$

which, apart from the integration over $\vec{r}$, is just half the value found in (B-2) above for $\bar{g} = 1$, when the integration with respect to $\vec{y}$ is taken over the whole space and not the half-space considered in our problem.

The error introduced by the use of (B-12), in place of the exact integral (B-11), is known to be small.

APPENDIX C

The Structure of the Large Eddies near the Wall in a Turbulent Boundary Layer

The work of Townsend[8,24] and of Grant[10] has shown that a relatively simple structure exists for the large eddies in a turbulent flow, or at least the experimental observations are not inconsistent with the hypothesis that the large scale motions can be adequately described in terms of relatively simple eddies. Grant's measurements of the $\bar{R}_{ij}(\vec{r})$ velocity correlations at different heights from the surface in a turbulent boundary layer give rise to the suggestion that the large eddies near the surface (i.e. in the constant stress layer) have the form of 'two-dimensional' jets of fluid originating near the viscous layer, and may arise from the instability of that layer, and are roughly aligned in the direction of mean motion. Similarly in the 'outer region' the large scale turbulent motion again appears to be dominated by the presence of mixing jets of turbulent fluid which originate in the interior of the flow and penetrate to the region of the non-turbulent flow outside the boundary layer.

A simple extension of the Townsend-Grant description of the large eddy structure for such motions led us to assume that the eddies randomly distributed over all space may be described by

$$u_1 = \frac{A}{\alpha_1}\left(1 - \alpha_3^2 x_3^2\right)\exp\left(-\frac{\alpha^2 x^2}{2}\right) \tag{C-1}$$

$$u_2 = -\frac{A}{\alpha_2}\alpha_1 x_1\left(1 - \alpha_3^2 x_3^2\right)\exp\left(-\frac{\alpha^2 x^2}{2}\right) \tag{C-2}$$

$$u_3 = \frac{A}{\alpha_3}\alpha_1\alpha_3 x_1 x_3\left(1 - \alpha_2 x_2\right)\exp\left(-\frac{\alpha^2 x^2}{2}\right) \tag{C-3}$$

where (u_1, u_2, u_3) are the components of velocity in the directions (x_1, x_2, x_3), with x_1 in the direction of the freestream and x_2 perpendicular to the wall, and

$$\alpha^2 x^2 \equiv \alpha_1^2 x_1^2 + \alpha_2^2 x_2^2 + \alpha_3^2 x_3^2 \tag{C-4}$$

The velocity components, given by Equation C-1 to C-3, satisfy the equation of continuity

$$\frac{\partial u_1}{\partial x_1} + \frac{\partial u_2}{\partial x_2} + \frac{\partial u_3}{\partial x_3} = 0 \tag{C-5}$$

with $(\alpha_1, \alpha_2, \alpha_3)$ having quite arbitrary values.

Following Townsend we next find the two-point velocity correlations are given by

$$R_{11}(\vec{r}) = \frac{A^2}{\alpha_1^3\alpha_2\alpha_3}\int d\vec{\bar{y}}\ (1 - \bar{y}_3^2)\ \{1 - (\bar{y}_3 + \bar{r}_3)^2\}\ \exp(-\bar{y}^2/2)\ \exp(-(\bar{y} + \bar{r})^2/2) \quad \text{(C-6)}$$

$$R_{22}(\vec{r}) = \frac{A^2}{\alpha_1\alpha_2^3\alpha_3}\int d\vec{\bar{y}}\ \bar{y}_1(\bar{y}_1 + \bar{r}_1)(1 - \bar{y}_3^2)\{1 - (\bar{y}_3 + \bar{r}_3)^2\}\exp(-\bar{y}^2/2)\ \times$$

$$\times\ \exp(-(\bar{y} + \bar{r})^2/2) \quad \text{(C-7)}$$

and

$$R_{33}(\vec{r}) = \frac{A^2}{\alpha_1\alpha_2\alpha_3^3}\int d\vec{\bar{y}}\ \bar{y}_1\bar{y}_3(\bar{y}_1 + \bar{r}_1)(\bar{y}_3 + \bar{r}_3)(1 - \bar{y}_2)(1 - \bar{y}_2 - \bar{r}_2)\ \times$$

$$\times\ \exp(-\bar{y}^2/2)\ \exp(-(\bar{y} + \bar{r})^2/2) \quad \text{(C-8)}$$

where $\bar{y}_1 = \alpha_1 y_1$; $\bar{y}_2 = \alpha_2 y_2$; $\bar{y}_3 = \alpha_3 y_3$ and $d\vec{\bar{y}} = d\bar{y}_1\ d\bar{y}_2\ d\bar{y}_3$.

After integration these relations can be written in the following form, if $\bar{R}_{11}$ etc., are the velocity correlation coefficients, and the subscript (b) denotes the big eddy contribution:

$$\bar{R}_{11}(\vec{r})_b = a_1(1 - \bar{r}_3^2 + \bar{r}_3^4/12)\ \exp(-\bar{r}^2/4) \quad \text{(C-9)}$$

$$\bar{R}_{22}(\vec{r})_b = a_2(1 - \bar{r}_1^2/2)\ (1 - \bar{r}_3^2 + \bar{r}_3^4/12)\ \exp(-\bar{r}^2/4) \quad \text{(C-10)}$$

$$\bar{R}_{33}(\vec{r})_b = a_3(1 - \bar{r}_1^2/2)\ (1 - \bar{r}_3^2/2)\ (1 - \bar{r}_2^2/6)\ \exp(-\bar{r}^2/4) \quad \text{(C-11)}$$

Grant's experimental results close to the wall suggest that

$$\frac{\alpha_3}{\alpha_2} \approx 2.2\ ;\quad \frac{\alpha_3}{\alpha_1} \approx 3.0\ ;\quad \frac{\alpha_2}{\alpha_1} \approx 1.35$$

whereas in the outer region

$$\frac{\alpha_3}{\alpha_2} \approx 0.6\ ;\quad \frac{\alpha_3}{\alpha_1} \approx 1.5\ ;\quad \frac{\alpha_2}{\alpha_1} \approx 2.5$$

Since

$$\left.\begin{aligned} R_{11}(o) &= \frac{\frac{3}{4}A^2\pi^{3/2}}{\alpha_1^3\alpha_2\alpha_3} \\ R_{22}(o) &= \frac{\frac{3}{8}A^2\pi^{3/2}}{\alpha_1\alpha_2^3\alpha_3} \end{aligned}\right\} \quad \text{(C-12)}$$

and

$$R_{33}(o) = \frac{\frac{3}{8} A^2 \pi^{3/2}}{a_1 a_2 a_3^3} \Bigg\} \tag{C-12}$$

we see that

$$\frac{\overline{u_{2_b}^2}}{\overline{u_{1_b}^2}} = \frac{a_1^2}{2a_2^2} \text{ and } \frac{\overline{u_{3_b}^2}}{\overline{u_{1_b}^2}} = \frac{a_1^2}{2a_3^2} \tag{C-13}$$

where $\overline{u_{1_b}^2}$ etc., represent the big eddy contribution to $\overline{u_1^2}$ etc. In the constant stress layer Laufer[9] finds that

$$\frac{\overline{u_3^2}}{\overline{u_1^2}} = 0.5 \quad \text{and} \quad \frac{\overline{u_2^2}}{\overline{u_1^2}} = \frac{1}{9}$$

whilst in the outer region

$$\frac{\overline{u_3^2}}{\overline{u_1^2}} = 0.5 \quad \text{and} \quad \frac{\overline{u_2^2}}{\overline{u_1^2}} = 0.2$$

This suggests that in the constant stress region

$$a_2 = 2.5\, a_1 \; ; \quad a_3 = 0.1\, a_1$$

whilst in the outer region

$$a_2 = 0.4\, a_1 \; ; \quad a_3 = 0.5\, a_1$$

These results show clearly that the role of the u_2 velocity component is changed in passing from the constant stress region to the outer region.

The simple eddy structure, in the constant stress region, portrayed by these results is that of an elongated vortex ring having its longest direction in line with that of the mainstream. It is rotating in a plane parallel to the wall, whilst the longitudinal motion is wavelike, being away from and then towards the wall. The latter motion is not unlike the jet-like motion described by Townsend and thus may similarly be interpreted. In the outer region the osculations are diminished in scale whilst the eddy spreads out slightly in a direction parallel to the wall and perpendicular to the freestream.

The complete value for $\bar{R}_{22}$ must be the sum of the contributions from the small and big eddies. Thus to $\bar{R}_{22}(\vec{r})_b$ we must add on $(1 - a_2)$ times the value for $\bar{R}_{22}(\vec{r})$ obtained from the smaller eddies. If we assume that these eddies are isotropic, in contrast with the strong anisotropy of the big eddies, we have that

$$\bar{R}_{22}(\vec{r})_s = (1 - a_2)\left[f + \frac{f'}{2} \frac{r_1^2 + r_3^2}{r} \right] \tag{C-14}$$

where f(r) is the longitudinal velocity correlation coefficient and $f' \equiv df/dr$. Thus finally

$$\bar{R}_{22} = \bar{R}_{22(s)} + \bar{R}_{22(b)} \tag{C-15}$$

On the assumption that

$$f(r) = \exp(-r/l) \tag{C-16}$$

the values of $\bar{R}_{22}$ have been evaluated and are compared with Grant's results in Figures 11, 12 and 13 for the measurements made close to the wall (i.e. $y/\delta \approx 0.08$). Although the agreement is not good quantitatively we have qualitatively obtained results which predict the basic form of the measured results. Similar comparisons can be made for $\bar{R}_{11}$ and $\bar{R}_{33}$ both in the constant stress layer and in the outer region provided the appropriate values of a_1, a_2 and a_3 are chosen as explained above.

With these values for $\bar{R}_{22}(\vec{r})$ we can now find the two-point pressure covariance on the wall, with zero time delay. From the previous analysis we find that the pressure covariance on the wall, with the separation vector $\vec{\xi}$, is given by

$$P(\vec{x}\ ;\ \vec{\xi}\ ;\ 0)_{\xi_2=0} = \frac{\rho^2}{\pi} < \tau_{12}^2\ \overline{u_2^2} > \int_{r_2>0} \bar{R}_{22}(\vec{r})\, \frac{\partial}{\partial \xi_1} \frac{(\xi_1 - r_1)}{|\vec{\xi} - \vec{r}|} \cdot d\vec{r} \tag{C-17}$$

and the corresponding spectrum function is

$$\pi(\vec{x}\ ;\ \kappa_1,\ 0,\ \kappa_3;\ 0) = \frac{\rho^2}{4\pi^3} < \tau_{12}^2\ \overline{u_2^2} > \int_{r_2>0} \bar{R}_{22}(\vec{r}) d\vec{r} \iint$$

$$\cdot\ e^{-i(\kappa_1 \xi_1 + \kappa_3 \xi_3)} \frac{\partial^2}{\partial r_1^2} |\vec{\xi} - \vec{r}|\ d\xi_1\ d\xi_3 \tag{C-18}$$

Thus if $\bar{P}(\vec{x}\ ;\ \kappa;\ 0)$ is the scalar wave number spectrum function on the surface found by averaging π over all angles in the plane, noting that $\kappa = \sqrt{\kappa_1^2 + \kappa_3^2}$ and

$$P(\vec{x}\ ;\ 0\ ;\ 0) = \int_0^\infty \bar{P}(\vec{x}\ ;\ \kappa\ ;\ 0)\ d\kappa \tag{C-19}$$

then

$$\bar{P}(\vec{x}\ ;\ \kappa\ ;\ 0) = \frac{\rho^2}{2\pi^2} < \tau_{12}^2\ \overline{u_2^2} > \int_0^{2\pi} \cos^2\theta\ d\theta \int_{r_2>0} d\vec{r}$$

$$\cdot\ \{e^{-\kappa r_2}(1 + \kappa\ r_2)\ \bar{R}_{22}(\vec{r})\ e^{-i(\kappa_1 r_1 + \kappa_3 r_3)}\} \tag{C-20}$$

since in Equation (C-18)

$$\iint e^{-i(\kappa_1\xi_1 + \kappa_3\xi_3)} \frac{\partial^2}{\partial r_1^2} |\vec{\xi} - \vec{r}| \, d\xi_1 \, d\xi_3 = 2\pi \frac{\kappa_1^2}{\kappa^3} (1 + \kappa r_2) \, e^{-\kappa r_2} \tag{C-21}$$

We can now find the separate contributions to $\bar{P}$ from the small and big eddies. Thus with $R_{22(b)}$ given by Equation (C-10) we find after some tedious though straightforward algebra that

$$\bar{P}(\vec{x} \; ; \; \kappa \; ; \; 0)_b = \frac{16 \, a_2 \, \rho^2 < \tau_{12}^2 \, \overline{u_2^2} > (a_1/a_3)^5 \, (a_1/a_2)}{a_1^3 (1 - (a_1/a_3)^2)^2} \times$$

$$\times \, (\kappa^3/a_1^3) \exp(-\kappa^2/2a_1^2) \exp(-\kappa^2/2a_3^2) \times I_2\left[\frac{\kappa^2}{2a_1^2}(1 - a_1^2/a_3^2)\right]$$

$$\left[1 + \sqrt{\pi} \, \frac{e^{\kappa^2/a_2^2} \, \mathrm{Erfc} \, (\kappa/a_2) \, (1 - 2\kappa^2/a_2^2)}{2 \, (\kappa/a_2)}\right] \tag{C-22}$$

Similarly with $R_{22(s)}$ given by Equation (C-14) with $f(r) = \exp(-r^2/l^2)$ (in order to simplify the algebra but not necessarily changing the order of magnitude of the results) we find that

$$\bar{P}(\vec{x} \; ; \; \kappa \; ; \; 0)_s = (1 - a_2) \, \rho^2 \, l^3 \frac{< \tau_{12}^2 \, \overline{u_2^2} >}{16} (\kappa l)^3 \, e^{-(\kappa l)^2/4} \times$$

$$\times \left[1 + \sqrt{\pi} \, \frac{e^{(\kappa l)^2/4} \, \mathrm{Erfc} \left(\frac{\kappa l}{2}\right) \left(1 - \frac{\kappa^2 \, l^2}{2}\right)}{(\kappa l)}\right] \tag{C-23}$$

A comparison between Equations (C-22) and (C-23) shows that whereas the small eddy contribution to $\bar{P}$ is dominant near wave numbers of $\kappa = l$ (the typical energy bearing scale of the smaller class of eddies) the big eddy contribution is very dependent on the relative scales of the big eddies in the directions (x_1, x_2, x_3) respectively, i.e. $1/a_1$, $1/a_2$, $1/a_3$.

Now in obtaining all these results it has been assumed that $R_{22}(\vec{r})$ does not change significantly with distance from the wall, which is certainly not true if, as we have shown above, we pass from the constant stress layer to the outer region. A rough comparison of Equation (C-22) with Willmarth's results[6] clearly shows that since high frequency peaks beyond $\kappa\delta_1 = 1$ (where δ_1 is the boundary layer displacement thickness) are not present, the pressure spectrum must be determined from the form of the velocity correlation function which is not too near the wall. This means in fact that a_3/a_1 cannot be large, or, in other words, the pressure spectrum is largely determined, up to the high frequency cut-off point, from the big eddy contributions with eddies whose transverse extent (in planes parallel with that of the wall) is not greatly different

from that in the streamwise direction. This would imply that the large eddies outside the constant stress region play a more significant role in the determination of the wall pressure fluctuations, than do the large eddies inside that region. This is not a result we might have expected from considerations of the region just outside the viscous layer in which the maximum values of the turbulent intensity and mean shear act. However, it must be borne in mind that our analysis is necessarily very approximate and the reason for this result might appear more obvious if we had worked through the analysis retaining the variable mean shear and turbulent intensity instead of replacing them by an averaged value taken over the entire shear layer.

Finally in this Appendix it is worth pointing out the differences which exist between our results and those of Kraichnan[5]. Kraichnan makes the assumption that the turbulence near the wall is homogeneous in planes parallel to the wall but not in planes normal to the wall. He next assumes a model for the turbulence in which 'mirror-like' velocity boundary conditions are satisfied on both sides of the wall. In this model the u_1 and u_3 velocity components are finite on the wall but u_2 is zero. The effective correlation coefficient is then taken as

$$\bar{R}_{22}(x_2,\ x_2';\ r_1,\ r_3) = \bar{R}_{22}(x_2 - x_2';\ r_1,\ r_3) - \bar{R}_{22}(x_2' + x_2;\ r_1,\ r_3) \qquad \text{(C-24)}$$

and when inserted into Equation (C-17) it leads to the result, if $f = \exp(-\sigma^2 r^2)$,

$$\bar{P}(\vec{x};\ \kappa;\ 0) \sim \left(\frac{\kappa}{\sigma}\right)^3 \exp\left(-\left(\frac{\kappa^2}{4\sigma^2}\right)\right) \sqrt{\pi}\ \frac{\left(1 + \frac{\kappa^2}{2\sigma^2}\right) \mathrm{Erfc}\left(\frac{\kappa}{2\sigma}\right) e^{\kappa^2/4\sigma^2}}{(\kappa/\sigma)} - 1 \qquad \text{(C-25)}$$

Numerically this result is very little different from that given by Equation (C-23) but is considered less satisfactory in view of the velocity boundary conditions being essentially different from those existing in the region outside the viscous layer. Kraichnan also includes the case of variable mean shear, following the law $\tau_{12} \sim \exp(-\beta x_2)$, and although this treatment is preferable to the averaged mean shear approach which we have adopted, the results are not qualitatively different and do not lead to an order of magnitude difference in the numerical results.

APPENDIX D

On Space-Time Correlations of the Fluctuating Velocity and Pressure

In the analysis above the pressure covariance has in the main been calculated for the case of zero time delay in axes fixed in the wall. However, in the detailed analysis the structure of the turbulence (i.e. $R_{22}(\vec{r})$) is required in a frame moving with the turbulence and it is not immediately obvious what the relations are between the turbulence in the moving and fixed frames. This problem will now be analysed below and the results compared with the experimental results of Favre[20] and Willmarth[6].

Let us consider a field of homogeneous turbulence in a frame of reference moving with the mean velocity $\bar{u}_p$ past the fixed point P. In this frame of reference the four-dimensional two point velocity correlation coefficient is

$$ {}^{(m)}\bar{R}_{ij}\ (\vec{r}') $$

where the four dimensional vector $\vec{r}'$ between the two points in the moving frame is given by

$$ \vec{r}' \equiv (r_1', r_2', r_3', r_4') $$

and r_4' is the co-ordinate representing the time delay. For example, if the longitudinal velocity correlation coefficient were given by

$$ f(\vec{r}') = \exp(-\alpha^2 r'^2) $$

where $$ \alpha^2 r'^2 = \alpha_1^2 r_1'^2 + \alpha_2^2 r_2'^2 + \alpha_3^2 r_3'^2 + \alpha_4^2 r_4'^2 $$

then alternatively

$$ f(\vec{r}') = \exp(-\sigma^2 r'^2)\ \exp(-\nu^2 \tau^2) \qquad \text{(D-1)} $$

where $1/\sigma$ is a measure of the eddy length and $1/\nu$ is a measure of its life time, and

$$ r'^2 = r_1'^2 + r_2'^2 + r_3'^2 $$

This result, although not general, is typical of the connection between space and time correlations.

In a stationary frame of reference $(\vec{r})$ in which the turbulence sweeps past at the speed $\bar{u}_p$ in the direction r_1, the relation between $\vec{r}'$ and $\vec{r}$ is

with $$ \vec{r}' \equiv (r_1', r_2', r_3'; \tau) \quad \text{and} \quad \vec{r} \equiv (r_1, r_2, r_3)\ , $$

$$ = \left(r_1 - \int_0^\tau \bar{u}_p\ (\tau')d\tau',\ r_2,\ r_3;\ \tau\right) \qquad \text{(D-2)} $$

We now make the hypothesis that the turbulence structure is unchanged in passing from fixed to moving co-ordinates. Thus with $\bar{u}_p$ independent of time, the velocity correlation coefficient in *fixed* areas

$$^{(f)}\bar{R}_{ij}(r_1 - \bar{u}_p \tau,\ r_2,\ r_3;\ \tau) = {}^{(m)}\bar{R}_{ij}(\vec{r}') \tag{D-3}$$

Examples

(i) Zero time delay $\tau = 0$

$$^{(f)}\bar{R}_{ij}(r_1,\ r_2,\ r_3;\ 0) = {}^{(m)}\bar{R}_{ij}(\vec{r}';\ 0) \tag{D-4}$$

This means that the spatial correlation of velocities in a fixed frame of reference equals those in a moving frame of reference.

(ii) Zero spatial separation in fixed axes $\vec{r} = 0$

$$^{(f)}\bar{R}_{ij}(-\bar{u}_p \tau,\ 0,\ 0;\ \tau) = {}^{(m)}\bar{R}_{ij}(r_1' = -\bar{u}_p \tau,\ 0,\ 0;\ \tau) \tag{D-5}$$

This means that the autocorrelation in a stationary frame is equivalent to a space ($r_1' = -\bar{u}_p \tau$) and time (τ) correlation in moving axes. This is *Taylor's hypothesis*, which is supported by Favres' [20] measurements in both free and shear flow turbulence.

(iii) Optimum time delay in fixed axes $r_1 = \tau_m \bar{u}_p$

$$^{(f)}\bar{R}_{ij}(0,\ 0,\ 0;\ \tau_m) = {}^{(m)}\bar{R}_{ij}(0,\ 0,\ 0;\ \tau = \tau_m) \tag{D-6}$$

This shows that the autocorrelation using an optimum time delay in fixed axes is equivalent to finding the autocorrelation in a moving frame of reference.

These three examples are made clearer by reference to a particular velocity correlation coefficient.

Suppose that in the moving frame

$$^{(m)}\bar{R}_{11}(r_1',\ 0,\ 0;\ \tau) = \exp(-\sigma^2 r_1'^2) \exp(-\nu^2 \tau^2) \tag{D-7}$$

then in case (i)

$$^{(f)}\bar{R}_{11}(r_1,\ 0,\ 0;\ 0) = \exp(-\sigma^2 r_1'^2)$$

$$= \exp(-\sigma^2 r_1^2) \tag{D-8}$$

showing clearly that no change of scale occurs in changing from fixed to moving axes.

In case (ii)

$$^{(f)}\bar{R}_{11}(-\bar{u}_p \tau,\ 0,\ 0;\ \tau) = \exp(-\sigma^2 \bar{u}_p^2 \tau^2) \exp(-\nu^2 \tau^2) \tag{D-9}$$

But in the moving frame ν is of the order of $\sigma\, u'$ (where u' is the turbulent intensity) so that if $u' << \bar{u}_p$

$$^{(f)}\bar{R}_{11}(-\bar{u}_p\,\tau,\ 0,\ 0;\ \tau) \approx \exp(-\sigma^2\,\bar{u}_p^2\,\tau^2) \tag{D-10}$$

which is equal to (D-8) if

$$r_1 = \bar{u}_p\,\tau \tag{D-11}$$

This result is the more usual form of expressing Taylor's hypothesis.

In case (iii)

$$^{(f)}\bar{R}_{11}(0,\ 0,\ 0;\ \tau_m) = \exp(-\nu^2\,\tau_m^2) \approx \exp\left(-\frac{u'^2}{\bar{u}_p^2}\cdot\sigma^2\bar{u}_p^2\,\tau_m^2\right) \tag{D-12}$$

This shows that the autocorrelation in the moving frame can be obtained from the autocorrelation in the fixed frame (by comparing (D-10) with (D-12)) by replacing the time delay (τ) in the fixed frame by

$$\tau = \frac{u'}{\bar{u}_p}\,\tau_m \tag{D-13}$$

The results of Favre[20] for both grid and wall turbulence (Fig.14), confirm this simple result provided that the time (τ_m) does not exceed roughly the times over which the autocorrelation in fixed axes are essentially non-zero.

Similar results might be expected to hold for the pressure covariance. Thus if we take the pressure autocorrelation in moving axes to be

$$^{(m)}P(0,0,0;\ \tau) = (1 - 2\nu^2\,\tau^2)\,\exp(-\nu^2\,\tau^2) \tag{D-14}$$

then we might expect that in moving axes

$$^{(m)}P(r_1',\ 0,\ 0;\ \tau) = (1 - 2\sigma^2\,r_1'^2)\,(1 - 2\,\nu^2\tau^2)\,\exp(-\sigma^2\,r_1'^2)\,\exp(-\nu^2\tau^2) \tag{D-15}$$

Therefore in case (i) above

$$^{(f)}P(r_1,\ 0,\ 0;\ 0) = (1 - 2\sigma^2\,r_1^2)\,\exp(-\sigma^2\,r_1^2) \tag{D-16}$$

In case (ii)

$$^{(f)}P(-\bar{u}_p\,\tau,\ \ 0,\ 0;\ \tau) \approx (1 - 2\sigma^2\bar{u}_p^2)\,\exp(-\sigma^2\bar{u}_p^2\,\tau^2) \tag{D-17}$$

This result cannot strictly apply to the pressure covariance at the wall for there $\bar{u}_p = 0$. However, if we assume that the turbulence is roughly convected over the

plane wall at some mean speed $\bar{u}_c$* then the autocorrelation in fixed axes is found from (D-17) with $\bar{u}_p$ replaced by $\bar{u}_c$.

In case (iii)

$$^{(f)}P(0,\ 0,\ 0;\ \tau_m) = \left(1 - 2\sigma^2 \frac{u'^2}{\bar{u}_c^2} \bar{u}_c^2 \tau_m^2\right) \times \exp\left(-\sigma^2 \frac{u'^2}{\bar{u}_c^2} \bar{u}_c^2 \tau_m^2\right) \qquad \text{(D-18)}$$

If we now consider the general case of a space-time correlation in fixed axes where $\tau \neq \tau_m$, the optimum time delay,

$$^{(f)}P(r_1 - \bar{u}_c \tau,\ 0,\ 0;\ \tau) = (1 - 2\sigma^2 \bar{u}_c^2 \alpha^2 \tau^2)\left(1 - 2\sigma^2 \frac{u'^2}{\bar{u}_c^2} \bar{u}_c^2 \tau^2\right) \times$$

$$\times \exp\left(-\sigma^2 \bar{u}_c^2 \tau^2\left(\alpha^2 + \frac{u'^2}{\bar{u}_c^2}\right)\right) \qquad \text{(D-19)}$$

where $\alpha = |r_1/\bar{u}_c \tau - 1|$

According to Willmarth[6], from measurements of the pressure fluctuations on wall turbulence we find that

$$\bar{u}_c \approx 0.8\ \bar{u}_1 \qquad \text{(D-20)}$$

where $\bar{u}_1$ is the freestream velocity. A comparison between Willmarth's results and those evaluated from

$$^{(f)}P(r_1 - \bar{u}_c \tau,\ 0,\ 0;\ \tau) = (1 - \sigma|r_1 - \bar{u}_c \tau|)\ (1 - \nu|\tau|) \times$$

$$\times \exp(-\sigma\ |\ r_1 - \bar{u}_c \tau\ |\ - \nu\ |\tau|) \qquad \text{(D-21)}$$

are shown in Figure 15. The agreement is good for small time delays (i.e. up to 0.5×10^{-3} secs., which is roughly the time for non-zero autocorrelation) but is poor at large time delays.

The reason for Willmarth's results being non-negative for large time-delays probably results from the growth of the eddies as they move downstream. For small time-delays this effect is small but as the time-delay is increased the eddy-life appears to be extended as a result of this growing scale of the moving turbulence.

---

*In incompressible flow the time variation of the pressure in fixed axes is the same as the time variation in the velocity. Thus the autocorrelation of the pressure in fixed axes must correspond to the autocorrelation of the velocity *averaged* over all angles. If then the turbulence has a dominant convection speed, this speed will also apply to the pressure autocorrelation.

APPENDIX E

The Evaluation of the Pressure Spectrum

It has been shown above that the pressure covariance at the point $\vec{x}$, with separation distance $\vec{\xi}$ on the wall is given by

$$P(\vec{x};\ \xi_1,\ 0,\ \xi_3;\ \tau) = \frac{\rho^2}{\pi} < \tau_{12}^2\ \overline{u_2^2} > \int_0^\infty dr_2 \int_{-\infty}^{\infty} dr_1 \int_{-\infty}^{\infty} dr_3\ \bar{R}_{22}(\vec{x};\ \vec{r};\ \tau) \times$$

$$\times \frac{r_2^2 + (r_3 - \xi_3)^2}{|\vec{\xi} - \vec{r}|^3} \qquad \text{(E-1)}$$

If the velocity correlation coefficient is given by

$$\bar{R}_{22}(\vec{r}';\ \tau) = e^{-\nu^2\tau^2}\ e^{-\ r'^2/l^2}\left[1 - \frac{r_3'^2 + r_1'^2}{l^2}\right] \qquad \text{(E-2)}$$

where $\vec{r}'$ is the separation vector in co-ordinates moving with the turbulence and we assume that the turbulence is convected with the constant speed u_c, then in fixed co-ordinates

$$\bar{R}_{22}(\vec{r};\ \tau) = e^{-\nu^2\tau^2}\ e^{-(r_2^2 + r_3^2)/l^2}\ e^{-(r_1 - u_c\tau)^2/l^2} \times$$

$$\times\ [1 - r_3^2/l^2 - (r_1 - u_c\tau)^2/l^2] \qquad \text{(E-3)}$$

If we write $\bar{r}_1 = r_1/l$ etc and $\bar{\nu} = \nu l/u_c$; $\bar{\tau} = u_c\tau/l$ then

$$P(\vec{x};\ 0;\ \tau) = \frac{4\rho^2}{\pi}\ l^2 < \tau_{12}^2\ \overline{u_2^2} > e^{-\bar{\nu}^2\ \bar{\tau}^2} \int_0^\infty d\bar{r}_1 \int_0^\infty d\bar{r}_2 \int_0^\infty d\bar{r}_3 \left(\frac{\bar{r}_2^2 + \bar{r}_3^2}{\bar{r}^3}\right)$$

$$[1 - \bar{r}_3^2 - (\bar{r}_1 - \bar{\tau})^2]\ e^{-\bar{r}_2^2 - \bar{r}_3^2}\ e^{-(\bar{r}_1 - \bar{\tau})^2} \qquad \text{(E-4)}$$

and the temporal spectrum function $\bar{P}(\vec{x};\ 0;\ \omega)$ is given by

$$\bar{P}(\vec{x};\ 0;\ \omega) = \frac{1}{2\pi} \int_{-\infty}^{\infty} e^{-i\omega\tau}\ P(\vec{x};\ 0;\ \tau)\ d\tau$$

$$= \frac{2\ \rho^2\ l^3 < \tau_{12}^2\ \overline{u_2^2} >}{\pi^2\ u_c} \int_0^\infty d\bar{r}_1 \int_0^\infty d\bar{r}_2 \int_0^\infty d\bar{r}_3 \left(\frac{\bar{r}_2^2 + \bar{r}_3^2}{\bar{r}^3}\right) \times \qquad \text{(E-5)}$$

$$\times\ e^{-(\bar{r}_2^2 + \bar{r}_3^2)} \int_{-\infty}^{\infty} e^{-i\bar{\omega}\bar{\tau}}\, e^{-\bar{\nu}^2\bar{\tau}^2}\, e^{-(\bar{r}_1 - \bar{\tau})^2} \times$$

$$\times\ [1 - \bar{r}_3^2 - (\bar{r}_1 - \bar{\tau})^2]\ d\bar{\tau} \qquad \text{(E-5)}$$

where $\bar{\omega} = \omega l/u_c$.

On taking the real part of E-5 we find that it reduces to

$$\frac{\bar{P}(\vec{x};\ 0;\ \omega)}{4\ \rho^2\ l^3 < \tau_{12}^2\ \overline{u_2^2} > /\pi^2 u_c} = \int_0^{\infty} d\bar{r}_1 \int_0^{\infty} d\bar{r}_2 \int_0^{\infty} d\bar{r}_3 \left(\frac{\bar{r}_2^2 + \bar{r}_3^2}{\bar{r}^3}\right) e^{-\left(\bar{r}_1^2 + \bar{r}_2^2 + \bar{r}_3^2\right)} \times$$

$$\times \int_0^{\infty} e^{-(\bar{\nu}^2 + 1)\bar{\tau}^2} \cos(\bar{\omega}\bar{\tau}) \left[(1 - \bar{r}_3^2 - \bar{r}_1^2 - \bar{\tau}^2)\cosh(2\ \bar{r}_1\ \bar{\tau})\right.$$

$$\left. +\ 2\ \bar{r}_1\ \bar{\tau}\ \sinh\ (2\ \bar{r}_1\ \bar{\tau})\right]\ d\bar{\tau} \qquad \text{(E-6)}$$

Now $\bar{\nu} \approx u'/u_c$ and is a small quantity (i.e. $\bar{\nu} << 1$). We can therefore neglect the term in $\bar{\nu}^2$ in Equation E-6.

Evaluation of

$$\int_0^{\infty} e^{-\bar{\tau}^2} \cos\ \bar{\omega}\ \bar{\tau}\ [(1 - \bar{r}_3^2 - \bar{r}_1^2 - \bar{\tau}^2)\ \cosh(2\ \bar{r}_1\bar{\tau}) + 2\ \bar{r}_1\bar{\tau}\ \sinh(2\ \bar{r}_1\bar{\tau})]\ d\bar{\tau} = I_1$$

This integral is reduced to 3 standard integrals which can be evaluated by the use of Fourier Transforms. Thus

$$I_1 = \int_0^{\infty} \cos\ \bar{\omega}\ \bar{\tau}\ e^{-\bar{\tau}^2}\ \cosh(2\ \bar{r}_1\bar{\tau})\ d\bar{\tau}\ (1 - \bar{r}_3^2 - \bar{r}_1^2)$$

$$- \int_0^{\infty} \cos\ \bar{\omega}\ \bar{\tau}\ e^{-\bar{\tau}^2}\ \cosh(2\ \bar{r}_1\bar{\tau})\ \bar{\tau}^2\ d\bar{\tau}$$

$$+ \int_0^{\infty} \cos\ \bar{\omega}\ \bar{\tau}\ e^{-\bar{\tau}^2}\ \sinh(2\ \bar{r}_1\bar{\tau})\ \bar{\tau}\ d\bar{\tau} \cdot 2\bar{r}_1$$

$$= \frac{\sqrt{\pi}}{2} e^{+\bar{r}_1^2}\ e^{-\bar{\omega}^2/4}\ \cos(\bar{r}_1\ \bar{\omega})\left\{\frac{1}{2} - \bar{r}_3^2 + \bar{\omega}^2/4\right\} \qquad \text{(E-7)}$$

Evaluation of

$$\int_0^\infty \frac{e^{-\bar{r}_1^2}}{\bar{r}^3} I_1 \, d\bar{r}_1 = I_2$$

From Equation E-7 we find that

$$I_2 = \frac{\sqrt{\pi}}{2} e^{-\bar{\omega}^2/4} \left\{ \frac{1}{2} - \bar{r}_3^2 + \bar{\omega}^2/4 \right\} \int_0^\infty \frac{\cos(\bar{r}_1 \bar{\omega}) \, d\bar{r}_1}{(\bar{r}_1^2 + \bar{r}_2^2 + \bar{r}_3^2)^{3/2}}$$

$$= \frac{\sqrt{\pi}}{2} e^{-\bar{\omega}^2/4} \left\{ \frac{1}{2} - \bar{r}_3^2 + \bar{\omega}^2/4 \right\} \bar{\omega} \frac{K_1(\bar{\omega} \sqrt{\bar{r}_2^2 + \bar{r}_3^2})}{\sqrt{\bar{r}_2^2 + \bar{r}_3^2}} \qquad \text{(E-8)}$$

Evaluation of

$$\int_0^\infty d\bar{r}_2 \int_0^\infty d\bar{r}_3 \, (\bar{r}_2^2 + \bar{r}_3^2) \, e^{-(\bar{r}_2^2 + \bar{r}_3^2)} \, I_2 = I_3$$

If we put $\chi = \sqrt{\bar{r}_2^2 + \bar{r}_3^2}$ and we use polar co-ordinates (χ, ϕ) in place of $(\bar{r}_2, \bar{r}_3)$ then, from Equation E-8,

$$I_3 = \frac{\sqrt{\pi}}{2} \bar{\omega} e^{-\bar{\omega}^2/4} \int_0^\infty \chi d\chi \int_0^\pi d\phi \left\{ \frac{1}{2} + \frac{\bar{\omega}^2}{4} - \chi^2 \cos^2\phi \right\}$$

$$\chi K_1(\bar{\omega}\chi) e^{-\chi^2}$$

$$= \frac{\pi^{3/2}}{2} \bar{\omega} e^{-\bar{\omega}^2/4} \int_0^\infty \chi^2 K_1(\bar{\omega}\chi) e^{-\chi^2} d\chi \left(\frac{1}{2} + \bar{\omega}^2/4 \right)$$

$$- \frac{\pi^{3/2}}{4} \bar{\omega} e^{-\bar{\omega}^2/4} \int_0^\infty \chi^4 K_1(\bar{\omega}\chi) e^{-\chi^2} d\chi$$

$$= \frac{\pi^{3/2}}{8} \bar{\omega}(1 + \bar{\omega}^2/2) \, e^{-\bar{\omega}^2/4} \int_0^\infty \sqrt{t} \, K_1(\bar{\omega}\sqrt{t}) \, e^{-t} \, dt$$

$$- \frac{\pi^{3/2}}{8} \bar{\omega}\, e^{-\bar{\omega}^2/4} \int_0^\infty t^{3/2} K_1(\bar{\omega}\sqrt{t})\, e^{-t}\, dt$$

$$= \frac{\pi^{3/2}}{32} \bar{\omega}^2 (1 + \bar{\omega}^2/2)\, \Gamma(-1, \bar{\omega}^2/4)$$

$$+ \frac{\pi^{3/2}}{32} \bar{\omega}^2 \left\{ \frac{4}{\bar{\omega}^2} e^{-\bar{\omega}^2/4} - 2(1 + \bar{\omega}^2/8)\, \Gamma(-1, \bar{\omega}^2/4) \right\}$$

$$= \frac{\pi^{3/2}}{8} e^{-\bar{\omega}^2/4} - \frac{\pi^{3/2}}{32} \bar{\omega}^2\, \Gamma(-1, \bar{\omega}^2/4)\, (1 - \bar{\omega}^2/4) \qquad \text{(E-9)}$$

If we combine the above results then from Equation (E-6)

$$\bar{P}(\vec{x};\, 0;\, \omega) = \frac{\rho^2\, l^3 < \tau_{12}^2\, \overline{u_2^2} >}{2\, \pi^{1/2}\, u_c} \left\{ \bar{\omega}^2/4 \cdot e^{-\bar{\omega}^2/4} - (\bar{\omega}^2/4)(1 - \bar{\omega}^2/4) \times \right.$$

$$\left. \times\ \mathrm{Ei}(-\bar{\omega}^2/4) \right\} \qquad \text{(E-10)}$$

We note finally that

$$P(\vec{x};\, 0) = 2 \int_0^\infty \bar{P}(\vec{x};\, 0;\, \omega)\, d\omega = \frac{2\, u_c}{l} \int_0^\infty \bar{P}(\vec{x};\, 0;\, \bar{\omega})\, d\bar{\omega}$$

$$= \frac{l^2 \rho^2}{\sqrt{\pi}} < \tau_{12}^2\, \overline{u_2^2} > \int_0^\infty d\bar{\omega} \left[\bar{\omega}^2/4\, e^{-\bar{\omega}^2/4} - (\bar{\omega}^2/4)(1 - \bar{\omega}^2/4)\, \mathrm{Ei}(-\bar{\omega}^2/4) \right]$$

$$= \frac{8}{15} l^2 \rho^2 < \tau_{12}^2\, \overline{u_2^2} > \qquad \text{(E-11)}$$

which is exactly double the value found by Kraichnan[11] for isotropic shear flow turbulence without boundaries, and provides an adequate check on the algebra leading to the spectrum function given by Equation (E-10). To allow for anisotropy a multiplying factor, $a \approx 1/3$, should be inserted into Equation E-11.

The spectrum function is plotted in Figure 4, where the abscissa is $(\omega\delta_1/\bar{u}_1)$. δ_1 is the boundary layer displacement thickness and $\bar{u}_1$ is the freestream velocity outside the shear layer. If we take $u_c = 0.8\, \bar{u}_1$, as given by Willmarth[6] and Harrison[7], and

$l/\delta_1 \doteq 2.4$ then

$$\frac{\omega \delta_1}{\bar{u}_1} = \frac{\bar{\omega}}{3} \tag{E-12}$$

If further we insert into (E-11) the crude estimate (based on Laufer's measurements of τ_{12} and $\sqrt{\overline{u_2^2}}$ and evaluated at the value of $u_\tau \delta/\nu = 1550$) $\delta_1^2/u_\infty^4 < \tau_{12}^2 \overline{u_2^2} > = 2 \times 10^{-5}$, and include the anisotropy factor of $a = 1/3$, then

$$\sqrt{\frac{\overline{P(\vec{x};\ 0)}}{\tfrac{1}{4} \rho^2 u_\infty^4}} = \frac{\sqrt{\overline{p^2}}}{\tfrac{1}{2} \rho u_\infty^2} = 9.3 \times 10^{-3}$$

compared with Willmarth's value of 0.006 and Harrison's value of 0.0095 under comparable conditions.

Similarly the peak value of $\bar{P}(\vec{x};\ 0;\ \omega)$, written in the form

$$\frac{2\ \bar{P}(\vec{x};\ 0;\ \omega)\ u_\infty}{\tfrac{1}{4} \rho^2 u_\infty^4\ \delta_1} \doteq 10^{-4}$$

whereas Willmarth obtained a value of 4×10^{-5} and Harrison a value of 6.3×10^{-5}.

It should be noted that our estimates are only 3 db higher than the measured values of Willmarth and give some support to our analysis. The inclusion of the anisotropy factor is justified by Kraichnan and was similarly used by Lilley[19] in evaluating the magnitude of the pressure fluctuations in the mixing region of a jet. Finally it might be noted that better agreement between theory and experiment might be expected, if the anisotropic form of the velocity correlation function were used, with its consequent improved scale relations to replace the ratio l/δ_1 as used above.

DISTRIBUTION

Copies of AGARD publications may be obtained in the various countries at the addresses given below.

On peut se procurer des exemplaires des publications de l'AGARD aux adresses suivantes.

BELGIUM BELGIQUE	Centre National d'Etudes et de Recherches Aéronautiques 11, rue d'Egmont, Bruxelles
CANADA	Director of Scientific Information Service Defense Research Board Department of National Defense 'A' Building, Ottawa, Ontario
DENMARK DANEMARK	Military Research Board Defense Staff Kastellet, Copenhagen Ø
FRANCE	O.N.E.R.A. (Direction) 25, Avenue de la Division Leclerc Châtillon-sous-Bagneux (Seine)
GERMANY ALLEMAGNE	Wissenschaftliche Gesellschaft für Luftfahrt Zentralstelle der Luftfahrtdokumentation Munchen 64, Flughafen Attn: Dr. H.J. Rautenberg
GREECE GRECE	Greek National Defense General Staff B. MEO Athens
ICELAND ISLANDE	Director of Aviation c/o Flugrad Reykjavik
ITALY ITALIE	Centro Consultivo Studi e Ricerche Ministero Difesa-Aeronautica Via dei Pontefici 3 Roma
LUXEMBURG LUXEMBOURG	Obtainable through Belgium
NETHERLANDS PAYS BAS	Netherlands Delegation to AGARD Kanaalstraat 10 Delft

NORWAY NORVEGE	Mr. O. Blichner Norwegian Defence Research Establishment Kjeller per Lillestrom
PORTUGAL	Direccao do Servico de Material da Forca Aerea Av. Antonio Augusto de Aguiar, 23-r/c Lisboa Attn: Lt. Col. Jose Pereira do Nascimento
TURKEY TURQUIE	Ministry of National Defence Ankara Attn. AGARD National Delegate
UNITED KINGDOM ROYAUME UNI	Ministry of Aviation T.I.L., Room 009A First Avenue House High Holborn London W.C.1
UNITED STATES ETATS UNIS	National Aeronautics and Space Administration (NASA) 1520 H Street, N.W. Washington 25, D.C.

Printed by Technical Editing and Reproduction Ltd
95 Great Portland St. London, W.1.

latter case an intensity many times that corresponding to the flow over a flat plate at zero pressure gradient, as typified by measurements on the wall of a wind tunnel. Experiments on a wall jet confirm these predictions and details of the few preliminary data are presented.

The results from the wall jet suggest that the intensity of the pressure fluctuations in the regions of adverse pressure gradient, on wings and bodies, approaching and beyond separation will be higher than in regions of zero pressure gradient.

Appendices are included which deal with the necessary extensions to the analysis to fit the velocity correlation functions as measured by Grant (1958), the effects of time delay and eddy convection.

This Report is one in the Series 253-284 of papers presented at the Boundary Layer Research Meeting of the AGARD Fluid Dynamics Panel held from 25th to 29th April, 1960, in London, England

latter case an intensity many times that corresponding to the flow over a flat plate at zero pressure gradient, as typified by measurements on the wall of a wind tunnel. Experiments on a wall jet confirm these predictions and details of the few preliminary data are presented.

The results from the wall jet suggest that the intensity of the pressure fluctuations in the regions of adverse pressure gradient, on wings and bodies, approaching and beyond separation will be higher than in regions of zero pressure gradient.

Appendices are included which deal with the necessary extensions to the analysis to fit the velocity correlation functions as measured by Grant (1958), the effects of time delay and eddy convection.

This Report is one in the Series 253-284 of papers presented at the Boundary Layer Research Meeting of the AGARD Fluid Dynamics Panel held from 25th to 29th April, 1960, in London, England

latter case an intensity many times that corresponding to the flow over a flat plate at zero pressure gradient, as typified by measurements on the wall of a wind tunnel. Experiments on a wall jet confirm these predictions and details of the few preliminary data are presented.

The results from the wall jet suggest that the intensity of the pressure fluctuations in the regions of adverse pressure gradient, on wings and bodies, approaching and beyond separation will be higher than in regions of zero pressure gradient.

Appendices are included which deal with the necessary extensions to the analysis to fit the velocity correlation functions as measured by Grant (1958), the effects of time delay and eddy convection.

This Report is one in the Series 253-284 of papers presented at the Boundary Layer Research Meeting of the AGARD Fluid Dynamics Panel held from 25th to 29th April, 1960, in London, England

latter case an intensity many times that corresponding to the flow over a flat plate at zero pressure gradient, as typified by measurements on the wall of a wind tunnel. Experiments on a wall jet confirm these predictions and details of the few preliminary data are presented.

The results from the wall jet suggest that the intensity of the pressure fluctuations in the regions of adverse pressure gradient, on wings and bodies, approaching and beyond separation will be higher than in regions of zero pressure gradient.

Appendices are included which deal with the necessary extensions to the analysis to fit the velocity correlation functions as measured by Grant (1958), the effects of time delay and eddy convection.

This Report is one in the Series 253-284 of papers presented at the Boundary Layer Research Meeting of the AGARD Fluid Dynamics Panel held from 25th to 29th April, 1960, in London, England

AGARD Report 276
North Atlantic Treaty Organisation, Advisory Group for Aeronautical Research and Development
ON SURFACE PRESSURE FLUCTUATIONS IN TURBULENT BOUNDARY LAYERS
G.M. Lilley and T.H. Hodgson
1960
38 pages, incl. 15 figs., 5 Appendices

Existing work on the pressure fluctuations in turbulent shear flows is briefly reviewed with special reference to the problem of wall turbulence.

An approximate theory for the pressure fluctuations on the wall under both a turbulent boundary layer and a wall jet is given and indicates in the

P.T.O.

3b2c2d:3b2e1a4a
532.526.4

AGARD Report 276
North Atlantic Treaty Organisation, Advisory Group for Aeronautical Research and Development
ON SURFACE PRESSURE FLUCTUATIONS IN TURBULENT BOUNDARY LAYERS
G.M. Lilley and T.H. Hodgson
1960
38 pages, incl. 15 figs., 5 Appendices

Existing work on the pressure fluctuations in turbulent shear flows is briefly reviewed with special reference to the problem of wall turbulence.

An approximate theory for the pressure fluctuations on the wall under both a turbulent boundary layer and a wall jet is given and indicates in the

P.T.O.

3b2c2d:3b2e1a4a
532.526.4

AGARD Report 276
North Atlantic Treaty Organisation, Advisory Group for Aeronautical Research and Development
ON SURFACE PRESSURE FLUCTUATIONS IN TURBULENT BOUNDARY LAYERS
G.M. Lilley and T.H. Hodgson
1960
38 pages, incl. 15 figs., 5 Appendices

Existing work on the pressure fluctuations in turbulent shear flows is briefly reviewed with special reference to the problem of wall turbulence.

An approximate theory for the pressure fluctuations on the wall under both a turbulent boundary layer and a wall jet is given and indicates in the

P.T.O.

3b2c2d:3b2e1a4a
532.526.4